

CAPITAL UNIVERSITY OF SCIENCE AND  
TECHNOLOGY, ISLAMABAD



**Immunoregulatory and  
Anti-Inflammatory Effects of  
Bioactive Compounds of Garlic  
Against Covid-19**

by

**Huma Ashraf**

A thesis submitted in partial fulfillment for the  
degree of Master of Science

in the

Faculty of Health and Life Sciences

Department of Bioinformatics and Biosciences

2021

Copyright © 2021 by Huma Ashraf

All rights reserved. No part of this thesis may be reproduced, distributed, or transmitted in any form or by any means, including photocopying, recording, or other electronic or mechanical methods, by any information storage and retrieval system without the prior written permission of the author.

*I dedicate this thesis to my parents and teachers*



## CERTIFICATE OF APPROVAL

### **Immunoregulatory and Anti-Inflammatory Effects of Bioactive Compounds of Garlic Against Covid-19**

by

Huma Ashraf

(MBS193038)

### THESIS EXAMINING COMMITTEE

S. No.	Examiner	Name	Organization
(a)	External Examiner	Dr. Sara Mumtaz	NUMS, Islamabad
(b)	Internal Examiner	Dr. Arshia Amin Butt	CUST, Islamabad
(c)	Supervisor	Dr. Erum Dilshad	CUST, Islamabad

---

Dr. Erum Dilshad

Thesis Supervisor

December, 2021

---

Dr. Sahar Fazal

Head

Dept. of Bioinfo. and Biosciences

December, 2021

---

Dr. M. Abdul Qadir

Dean

Faculty of Health and Life Sciences

December, 2021

## *Author's Declaration*

I, **Huma Ashraf** hereby state that my MS thesis titled “**Immunoregulatory and Anti-Inflammatory Effects of Bioactive Compounds of Garlic Against Covid-19**” is my own work and has not been submitted previously by me for taking any degree from Capital University of Science and Technology, Islamabad or anywhere else in the country/abroad.

At any time if my statement is found to be incorrect even after my graduation, the University has the right to withdraw my MS Degree.

**(Huma Ashraf)**

Registration No: MBS193038

## *Plagiarism Undertaking*

I solemnly declare that research work presented in this thesis titled “**Immunoregulatory and Anti-Inflammatory Effects of Bioactive Compounds of Garlic Against Covid-19**” is solely my research work with no significant contribution from any other person. Small contribution/help wherever taken has been duly acknowledged and that complete thesis has been written by me.

I understand the zero tolerance policy of the HEC and Capital University of Science and Technology towards plagiarism. Therefore, I as an author of the above titled thesis declare that no portion of my thesis has been plagiarized and any material used as reference is properly referred/cited.

I undertake that if I am found guilty of any formal plagiarism in the above titled thesis even after award of MS Degree, the University reserves the right to withdraw/revoke my MS degree and that HEC and the University have the right to publish my name on the HEC/University website on which names of students are placed who submitted plagiarized work.

**(Huma Ashraf)**

Registration No: MBS193038

## *Acknowledgement*

All the praises are to be for Almighty ALLAH and prophet MUHAMMAD (SAW). I would like to express my wholehearted thanks to my family for the generous support throughout of pursuing the MS degree. I am heartily grateful to my supervisor Dr. Erum Dilshad (Assistant professor, Department of Bioinformatics & Biosciences, CUST) for her kind support, guidelines and arrangement of tutorial classes. I especially say thanks to Dr. Naeem Mahmood Ashraf (Lecturer Biochemistry & Biotechnology, University of Gujrat) for his assistance on computational approaches.

Thanks to all.

**(Huma Ashraf)**

---

## *Abstract*

An outbreak of pneumonia occurred on December 2019 in Wuhan city of China that caused serious public health emergency by spreading around the globe. Finally, it was officially announced on 9 January 2020 that the outbreak in Wuhan is caused by novel corona virus 2019-nCoV. Globally people become more concern to use natural products over synthetic ones. That's why this research was designed to discover potential antiviral compounds from *Allium sativum* and selected ligands are 3-(Allylsulphinyl)-L-alanine, Allicin, Diallyl sulfide, Diallyl disulfide, Diallyl trisulfide, Glutathione, L-Cysteine, S-allyl-mercapto-glutathione, Quercetin, Myricetin, Thiocysteine, Gamma-glutamyl-Lcysteine, Gamma-glutamylallyl-cysteine, Fructan, Lauricacid, Linoleicacid, Allixin, Ajoene, Diazinon Kaempferol, Levamisole, Caffeicacid, Ethyl linoleate, Scutellarein, and S-allylcysteine methyl-ester were selected. Virtual screening of these ligands was carried out against drug targets by CB-dock. The motive of the present research is to discover potential antiviral components from *Allium sativum*. Twenty-five phyto compounds (which represent almost all classes of natural antiviral compounds) are selected from literature and databases. Physicochemical and Pharmacokinetics properties determine the final destiny of compounds as drug or non-drug compounds. Best five compounds on the basis of primary and secondary filters, toxicity predicted values and binding score are Allicin, Diallyl Sulfide, Diallyl Disulfide, Diallyl Trisulfide, Ajoene and Levamisole which showed themselves as hit compounds. Further refining by screening filters represents Levamisole as a lead compound. All the interaction visualization analysis studies are performed by PyMol molecular visualization tool and LIGPLOT+. Finally, as a result of this study, Levamisole was identified as a most potential antiviral compound which might be a drug candidate to treat SARS-CoV-2 in future. However further research is necessary to investigate potential medicinal use.

**Keywords:** SARS-CoV-2, *Allium sativum*, Molecular Docking, Lead Compounds, Allicin, Diallyl Sulfide, Diallyl Disulfide, Diallyl Trisulfide, Ajoene and Levamisole.



# Contents

<b>Author's Declaration</b>	<b>iv</b>
<b>Plagiarism Undertaking</b>	<b>v</b>
<b>Acknowledgement</b>	<b>vi</b>
<b>Abstract</b>	<b>vii</b>
<b>List of Figures</b>	<b>xi</b>
<b>List of Tables</b>	<b>xiii</b>
<b>Abbreviations</b>	<b>xiv</b>
<b>1 Introduction</b>	<b>1</b>
1.1 Problem Statement . . . . .	3
1.2 Aims and Objectives . . . . .	4
<b>2 Literature Review</b>	<b>5</b>
2.1 Structural Features and Origin of Corona Viruses . . . . .	5
2.2 Mechanism of SARS-CoV-2 Entry in Cells . . . . .	6
2.3 Medicinal Plants . . . . .	9
2.4 Garlic . . . . .	10
2.4.1 Bioactive Compounds of Garlic . . . . .	11
2.5 Molecular Docking Studies . . . . .	11
2.6 Covid Proteins . . . . .	12
2.6.1 NSP13 . . . . .	12
2.6.2 S Protein . . . . .	12
2.6.3 N Protein . . . . .	12
<b>3 Materials and Methods</b>	<b>13</b>
3.1 Selection of Disease . . . . .	13
3.2 Selection of Protein . . . . .	14
3.3 Primary Sequence Retrieval . . . . .	14
3.4 Analysis of Physiochemical Properties . . . . .	14

---

3.5	Identification of Functional Domains	15
3.6	Active Site Identification	15
3.7	Ligand Preparation	15
3.8	Bioactivity Analysis of Ligands and Toxicity Measurement	15
3.9	Molecular Docking Process	16
3.10	Visualization of Ligand/Protein via PyMol	16
3.11	Analysis of Docked Complex via LigPlot	16
3.12	Ligand ADMET Properties	16
3.13	Active Inhibitor Identification	17
3.14	FDA Approved Drug-Proposed Antioxidant Agent Comparison	17
<b>4</b>	<b>Results and Discussion</b>	<b>18</b>
4.1	Target Proteins from UniProt	18
4.1.1	Primary Sequence Retrieval	18
4.1.2	3D Structure Predictions of Protein	20
4.2	Functional Domain Identification of Proteins	22
4.2.1	Ligand Selection	24
4.3	Molecular Docking	25
4.4	Interaction of Ligands and Target Protein	27
4.5	ADMET Properties of Ligands	41
4.5.1	Pharmacodynamics	41
4.5.2	Pharmacokinetics	42
4.6	Absorption	43
4.7	Distribution	44
4.8	Metabolism	46
4.9	Excretion	48
4.10	Toxicity Prediction	49
4.11	Lead Compounds Identification	52
4.12	Drug Identification Against Covid-19	53
4.12.1	Remdesivir	53
4.13	Drug ADMET Properties	54
4.13.1	Toxicity prediction of Reference Drug	54
4.13.2	Absorption Properties	55
4.13.3	Distribution Properties	55
4.13.4	Metabolic Properties	56
4.13.5	Excretion Properties	56
4.14	Remdesivir Mechanism of Action	56
4.15	Remdesivir Molecular Docking	57
4.16	Remdesivir Comparison with Lead Compound	58
4.17	ADMET Properties Comparison	59
4.17.1	Toxicity Comparison	59
4.17.2	Absorption Properties Comparison	60
4.17.3	Metabolic Properties Comparison	61
4.17.4	Distribution Properties Comparison	62

---

4.17.5 Excretion Properties Comparison . . . . .	62
4.18 Physiochemical Properties Comparison . . . . .	63
4.19 Docking Score Comparison . . . . .	64
<b>5 Conclusion and Future Prospects</b>	<b>65</b>
<b>Bibliography</b>	<b>77</b>
<b>Appendix A</b>	<b>77</b>
<b>Appendix B</b>	<b>81</b>
<b>Appendix C</b>	<b>87</b>

# List of Figures

2.1	(A): Structure and genome organization of SARS-CoV-2 [27]. . . . .	6
2.2	Elements in immunological profiles of patients with COVID-19 infection [29]. . . . .	7
2.3	Mechanism of SARS-CoV-2 entry in cells. (A) Binding of SARSCoV-2 spike to the host ACE2 receptor. (B) Cleavage of SARS-CoV-2 spike by TMPRSS2, membrane fusion, infection, and viral RNA release into the host cell [34]. . . . .	8
2.4	Garlic ( <i>Allium sativum</i> ), Garlic plant, Garlic oil and Garlic powder [39]. . . . .	10
3.1	The flow chart of methodology. . . . .	13
4.1	Fasta sequence and structure of nucleoprotein (target protein) [62].	19
4.2	Structure and Fasta Sequence of Spike Protein (Target Protein) [62].	19
4.3	Structure and Fasta Sequence of Helicases (Target Protein) [62]. . .	20
4.4	Structure of SARS-CoV-2 3CL protease (3CL pro) protein [63]. . .	21
4.5	Conserved domains of target protein [67]. . . . .	22
4.6	Functional domains of target protein [68]. . . . .	23
4.7	Interactions of Ajoen with target protein obtained By Ligplot. . . .	28
4.8	Interactions of Allixin with target protein obtained By Ligplot. . . .	28
4.9	Interactions of diallyl disulfide with target protein obtained By Ligplot. . . . .	29
4.10	Interactions of linoleate with target protein obtained By Ligplot. . .	29
4.11	Interactions of Gamma-Glutamyl-S-Allylcysteine with target protein obtained By Ligplot. . . . .	30
4.12	Interactions of lauric acid with target protein obtained by ligplot. . .	30
4.13	Interactions of l-cystein with target protein obtained by ligplot. . .	31
4.14	Interactions of Myrecetin with target protein obtained by ligplot. . .	31
4.15	Interactions of 3-(Allylsulphinyl)-L-Alanine with target protein obtained by ligplot. . . . .	32
4.16	Interactions of allicin with target protein obtained by ligplot. . . . .	32
4.17	Interactions of caffeic acid with target protein obtained by ligplot. . .	33
4.18	Interactions diallyl sulfide with target protein obtained by ligplot. . .	33
4.19	Interactions of diazinon with target protein obtained by ligplot. . .	34
4.20	Interactions of fructan with target protein obtained by ligplot. . . .	34

---

4.21 Interactions of Gamma-Glutamyl-L-Cysteine with target protein obtained by ligplot. . . . .	35
4.22 Interactions of Lauric acid with target protein d obtained by ligplot.	35
4.23 Interactions of Levamisole with target protein obtained by ligplot. .	36
4.24 Interactions of Linoleic acid with target protein obtained by ligplot.	36
4.25 Interactions of quercetin with target protein obtained by ligplot. . .	37
4.26 Interactions of S-allylcysteine methylester with target protein obtained by ligplot. . . . .	37
4.27 Interactions of S-allyl-mercapto-glutathione with target protein obtained by ligplot. . . . .	38
4.28 Interactions of scutellarein with target protein obtained by ligplot. .	38
4.29 Interactions of glutathionine with target protein obtained by ligplot.	39
4.30 Interactions of thiocysteine with target protein obtained by ligplot.	39
4.31 Interactions of kaomferol with target protein obtained by ligplot. .	40
4.32 Interactions of diallyl trisulfide with target protein obtained by ligplot.	40
4.33 Mechanism of Action of Remdesivir Drug. . . . .	57

# List of Tables

4.1	Area and volume of the obtained pockets by CASTp [68]	23
4.2	Results of CB dock [82, 83].	26
4.3	ADMET properties (lipaski's rule of five) [79].	42
4.4	Distribution properties of ligands [89].	45
4.5	Parameters measuring metabolism of ligands [87].	46
4.6	Excretion properties of ligands [89].	48
4.7	Predicts toxicity of ligands [93].	50
4.8	Toxicity properties of Remdesivir	54
4.9	Absorption properties of Remdesivir	55
4.10	Distribution properties of Remdesivir	55
4.11	Metabolic properties of Remdesivir	56
4.12	Excretion properties of Remdesivir	56
4.13	Docking result of Remdesivir	58
4.14	Remdesivir comparison with lead compound	58
4.15	Comparative values of toxicity of Remdesivir and Levamisole	60
4.16	Comparative values of absorption of Remdesivir and Levamisole	61
4.17	Comparative values of metabolic properties of Remdesivir and Levamisole	61
4.18	Comparative values of distribution of Remdesivir and Levamisole	62
4.19	Values of excretory properties of Remdesivir and Levamisole.	63
4.20	Comparison of physiochemical properties of Remdesivir and Levamisole	63
4.21	Docking Score Comparison	64
1	Ligands name, molecular formula, weight, and molecular structure [71].	77
2	Ligands, hydrogen bonds, hydrophobic interactions obtained by ligplot [72, 73].	81
3	Absorption among different ligands [86].	87

# Abbreviations

<b>COVID-19</b>	Coronavirus Disease
<b>CoVs</b>	Corona Viruses
<b>GM</b>	Genetically Modified
<b>MERS</b>	Middle East respiratory syndrome
<b>RNA</b>	Ribonucleic Acid
<b>SARS</b>	Severe Acute Respiratory Syndrome
<b>WHO</b>	World Health Organization

# Chapter 1

## Introduction

An outbreak of pneumonia pandemic was occurred in the month of December 2019 in China that caused serious public health emergency by spreading around the globe [1]. Finally, it was officially announced on 9 January 2020 that the outbreak in Wuhan is caused by novel corona virus 2019-nCoV [2, 3]. The unique corona virus was named as Severe Respiratory Disease. Corona viruses (CoVs) are responsible for causing infection in humans and as well as in animals and they cause different many diseases and disorders related to respiratory issues basically. These spreaded viruses are grouped into, alpha, beta, gamma and delta variants. In Homo sapiens the upper respiratory infections are mostly done by alpha and beta corona viruses whereas, rarely lower respiratory tract infections are seen [4]. Pandemic arises nearly 2002–2003 from China and Asia Pacific regions was caused by SARS-CoV that infected more than 8000 people around the globe with 10% mortality rate [7, 8].

Fever, cough and lowering of oxygen level in blood were the common symptoms that were seen in patients suffering from illness [9]. For the very first time in 2012 (MERS-CoV) was reported from kingdom of Saudi Arabia, basically it's a 2C beta CoV [10]. Severe pneumonia and renal failure was caused by MERS-CoV [11]. The sequence similarity of SARS-CoV-2 virus is nearly 80% with SARS-CoV virus but corona virus is much severe and dangerous [12]. On 11 March, COVID-19 was declared as pandemic disease by WHO as it is easily transferable from one to



another human. By July 2021, globally 100 million confirmed cases of COVID-19 were reported with more than 2 million deaths. It can cause death in severe cases [13]. It was revealed when Whole genome sequencing is done that corona virus is more related to bat CoV RaTGI3 with 96.2% sequence similarity [14].

The virus transmits by contact in any form from one to another human being i.e., direct or indirect contact [15]. Approximately 2-14 days are the incubation period of the virus. Following are the symptoms which may present in infected people: fever, dry cough, and lowering of oxygen level in blood. Moreover, few infected people are asymptomatic means no symptoms of disease were shown in them. COVID-19 is mostly not so severe, sometimes patients are having health issues like hypertension, diabetes, immunodeficiency, etc. [16]. For such patients, a multi-organ failure may occur in case of severe condition which can cause death.

Globally, for the treatment of COVID-19, without having proof of inflammations role in the cure of the illness, so many immune modulators, for example glucocorticoids and anti-inflammatory therapies are being used for this purpose. The major determinant in the Host survival is dependent on the host's ability to clear the viral infection in the lung provides a vital advantage to the host by aiding effective viral clearance [17]. Pathophysiological mechanism of COVID-19 is not well understood, several evidences have revealed that COVID-19 infected patients have high levels of cytokine and referred as cytokine storm or cytokine release syndrome. This abnormal rise in cytokine level is considered as severe decline of health conditions in the infected patients [19]. Thus, the severity of disease in infected patients of COVID-19 can be reduced during by suppressing elevated inflammatory response [20].

Many drugs are available in the market against SARS-CoV-2 but one cannot say which one is perfect from all the above drugs. Herbal medicines can be used as a antiviral against different infections which are caused by SARS-CoV-2 [21]. Basically, medicinal plants are those plants in which healing properties are present and they show detrimental effects medicinal effects on the human or animal body. These plants can be used for the synthesis of various drugs since they possess

various medicinal compounds. Leaf, seeds, root, flower or even whole plant of medicinal plants are used for the development of drugs. Medicinal plants have therapeutic effects due to the presence of bioactive compounds that work as medicinal agents. Therefore, worldwide these plants are used as complementary or alternative medicine [22]. The secondary metabolites that are present in the medicinal plants can prevent viral penetration and replication by binding with viral proteins and enzymes. Herbal medicines may be toxic, if they are consumed without the appropriate dosage. The genetically modified (GM) plants results in toxins or allergens and can cause serious health issues because they can cause unnatural change in naturally occurring protein or the metabolic pathways [23]. Therefore, the selection of proper medicinal plants is also very important. Plants contain a lot of bio-active compounds and essential oils which is beneficial for human health. So, these plants and spices contain special compounds which prevent various diseases. Another factor that increased the demand of chemical free herbal drugs was the toxic and adverse effect of allopathic medicines. But the distribution of medicinal plants is not same worldwide and usually medicinal herbs are collected from wild life populations [21]. Moreover, the demand for wild life resources in Europe, North America and Asia has increased from 8 to 15% per year. Medicinal plants have a promising future as long as they exist. Nearly half a million plants worldwide are yet not studied in medical practice so, current and future studies on medicinal plants may be effective for the treatment of chronic diseases. Naturally occurring spices and their isolated active components have been reported for targeting the both inflammatory and anti-inflammatory pathways and inducing anti-inflammatory effects in several life threatening ailments. Spices and herbs are thought to be excellent immunity boosters, therefore they are prevalently used in Asian countries [23].

## 1.1 Problem Statement

Although many drugs are available against SARS-CoV-2 but they don't give accurate results, currently there are no proven remedies so some new herbal medicine

needs to be discovered that will have low side effects instead of synthetic ones and that will cure the disease and also show less side effects [20].

## **1.2 Aims and Objectives**

The aim of the present study is to identify Immunomodulatory and Anti-Inflammatory effects of bioactive compounds of Garlic. Therefore, we focus on protein-ligand interactions, which play a significant role in structural drug design.

1. To analyze the binding conformation between targeted proteins of Covid-19 of garlic as standard immunomodulatory and anti-inflammatory agents.
2. To study the interaction between targeted proteins and the selected ligands.

# Chapter 2

## Literature Review

### 2.1 Structural Features and Origin of Corona Viruses

The corona viruses are positive-stranded single RNA viruses, having 20-30 kb genomic length approximately [26]. These viruses are the member of to the coronaviridae family of the order nidovirales.

They are further subdivided into four genera – alpha ( $\alpha$ ), beta ( $\beta$ ), gamma ( $\gamma$ ), and delta ( $\delta$ ) corona virus [27]. The  $\alpha$ - and  $\beta$ -CoVs infects humans as well as animal. Some examples of  $\alpha$ -CoV are the HCoVs such as 229E, NL63etc, whereas  $\beta$ -CoVs consists of the OC43, HKU1, SARS-CoV, MERS-CoV, and SARS-CoV-2. The avian coronaviruses belongs to  $\gamma$ - and  $\delta$ -CoVs [26].

Four important structural proteins are encoded by viral genome of CoV [27]. In the lipid bilayer of the viral envelope the E, S, and M proteins are anchored [28]. The shape to the virus is given by M protein that is approximately 25-30 kDa. Virus is released by E protein that is approximately 8-12 kDa. M and E proteins are responsible for viral assembly and for the facilitation of maturation of viral envelopes. The function of N protein is to form the nucleocapsid by binding with the viral genome to promote viral packaging [29].

The S protein is also known as class I fusion protein and the function of S protein is to create spike like protrusions on the virus. The length of S protein is approximately 150 kDa. It consists of S1 and S2 subunits that are formed by the cleavage in the host. The cell membrane of the host fuses with the S2 subunit leading to the entry of virus into the host cells. The structure and genome of SARS-CoV-2 is shown in Figure 2.1 [26-28].

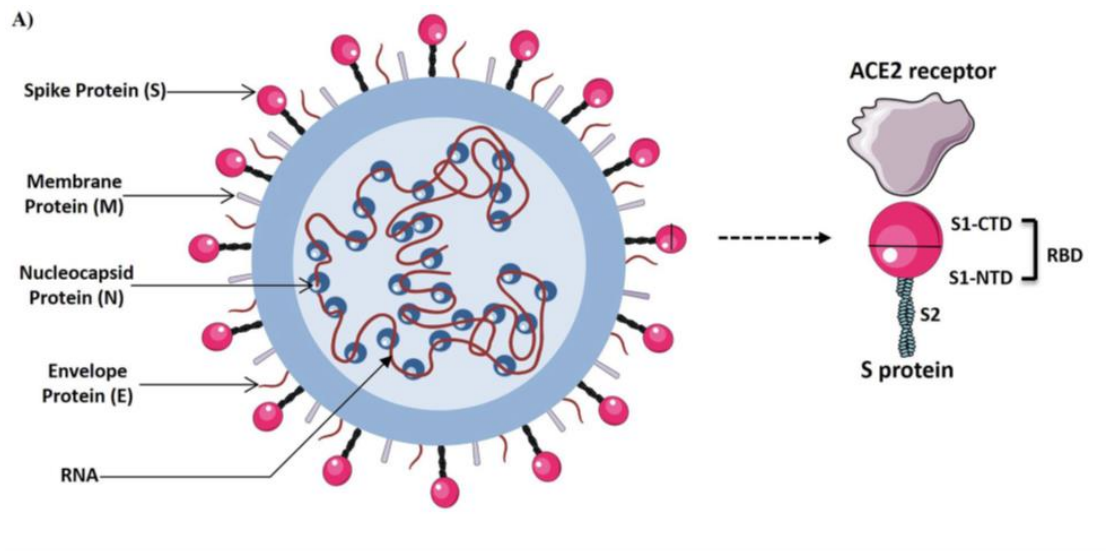


FIGURE 2.1: (A): Structure and genome organization of SARS-CoV-2 [27].

## 2.2 Mechanism of SARS-CoV-2 Entry in Cells

The mechanism of SARS-COV-2 infection is not completely elucidated till now. To unravel the mechanism of infection and pathogenesis of the novel coronavirus globally several studies are being conducted on SARS-COV-2. The  $\beta$ -CoVs- SARS-CoV and SARS-CoV-2 infect humans and are identical to each other. The attachment and fusion of the virus with the host cell is contributed by the S protein. The viral infection is initiated by the binding RBD of the S1 subunit of S protein to the host cell receptor. Studies have revealed that human ACE2 (hACE2) receptor is used by SARS-CoV and SARS-CoV-2 for their attachment to the host cells. The significant expression of ACE2 receptor is in the type II alveolar, oral mucosal, and nasal epithelial cells [29].

These organs like kidney, heart, respiratory airways and cornea are mostly affected in COVID-19 since they are highly vulnerable. Figure 2.2 shows effects of Covid-19 infection in the patients.



FIGURE 2.2: Elements in immunological profiles of patients with COVID-19 infection [29].

A Research revealed that corona virus has less capacity to bind with the hACE2 receptor as compared to SARS-CoV. It also concluded more capacity with the hACE2 receptor was due to structural changes in the ACE2-binding ridge of SARS-CoV-2RBD [30, 31]. Pre-activation of the S protein occurs due to this cleavage that further leads to the promotion of the subsequent type II transmembrane serine protease (TMPRSS2)-dependent viral entry into host cells. TMPRSS2 is considered significant. According to the reports, TMPRSS2 is expressed broadly into the lungs, colon, kidney, heart, pancreas and the nasal cavity. Moreover, the epithelial cells of nasal cavity are enriched with ACE2 receptor and TMPRSS2 [32]. Other than that, the ACE2 receptor is also cleared by this conformational change [33].

According to research usually TMPRSS2 is expressed in the ACE2+ cell types. Moreover, in > 70–90% of ACE2+ cells, the expression of proteases such as cathepsin B (Cat B) was seen [33]. It was also concluded that SARS-CoV-2 could enter

by utilizing alternative routes into the host cell. In another in vitro study, almost similar results were obtained which revealed the dependency of SARS-CoV-2 for priming and entering into the host cell on Cathepsin B/L (CatB/L) and TMPRSS2. Moreover, it was further concluded that partial inhibition of viral entry occurs because of inhibition of any one of these proteases. During this in vitro study it was found that in order to enter the host cell the virus may utilize CatB/L if TMPRSS2 is not present as shown in the Figure 2.3 [34].

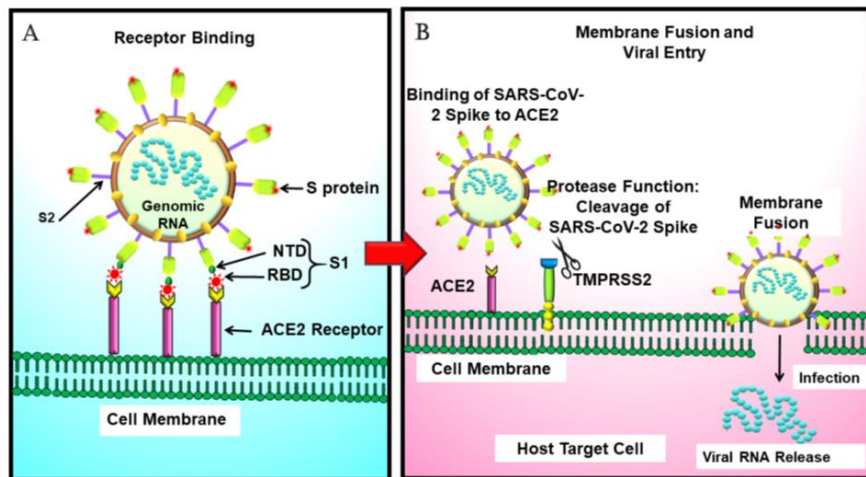


FIGURE 2.3: Mechanism of SARS-CoV-2 entry in cells. (A) Binding of SARSCoV-2 spike to the host ACE2 receptor. (B) Cleavage of SARS-CoV-2 spike by TMPRSS2, membrane fusion, infection, and viral RNA release into the host cell [34].

The genomic material was liberated in the cytoplasm after the entry of SARS-CoV-2 which further controls the host's machinery that is used for protein synthesis and leads to the translation of the mRNA in the nucleus. Moreover, synthesizes of the viral proteins by utilizing the machinery of host to initiates viral replication [31]. After two weeks, some patients experience many complications which may include failure of respiratory system following by sudden decline in the health of patient, decline in lymphocytes number for example in peripheral blood natural killer cells are present, pro inflammatory cytokine storm, atrophy of lymph nodes and spleen.

With the passage of time more and more solutions will be learned by medical community but for time being this is the solution [35]. The critical condition regarding

corona virus is well played by inflammatory response. After SARSCoV2 entry into the host body's immune system is triggered, which results in the reduced lung capacity and functional impairment if uncontrolled [36]. Throughout the course of the disease, response of inflammatory system has vital role since it leads to the pulmonary interstitial arteriolar walls damage. Other than this, some nonspecific responses have been detected for example, alveolar epithelial cells severe exfoliation, alveolar space infiltration, inflammatory and edema cellin filtration, alveolar septa damage and alveolar septal widening [35, 36].

Basically, immune responses and immunopathology SARS-CoV-2 infection is categorized as following three stages; symptomatic one, the non-severe symptomatic and lastly the severe respiratory symptomatic phase. These complications may leads to multi organ failure. In some patients injury of pulmonary occurs, ARDS, viral sepsis and complications like failure of organs and even death may be triggered [38, 39].

Till now for the mitigation of Covid-19 certain strategies have been found more effective worldwide consisting rise the standard of public health practices, for example hand washing with soap on regular basis after proper interval of time, use of face mask in a proper manner, and covering a cough with elbow and also take care of social distance which should be helpful in controlling this pandemic etc. Moreover, it is also concluded that healthy nutritional status may support immune function and prevent severe and further infection [40].

## 2.3 Medicinal Plants

Globally, we have been bestowed with a variety of the medicinal plants which help in curing many diseases. Other than that these plant based products are high in nutrition, also they are also rich in therapeutic properties. Different parts of plants have many different phytochemical and natural compounds that from have been a part of traditional medicine for ages and consumed for various health benefits [41, 42].



## 2.4 Garlic

Clinical trials and investigation showed the potency of garlic extracts and its supplements against many diseases. It has been showed that significant anti-inflammatory has been shown by the spice. Supplementation of 3.6 g aged garlic extracts (AGE) daily was found to diminish the serum levels of TNF- $\alpha$  and IL-6 in obese adults, thus lessening the risk of occurrence of multiple inflammatory chronic diseases associated with obesity. Garlic extract supplementation also relieved pain and other clinical symptoms associated with knee osteoarthritis [40].



FIGURE 2.4: Garlic (*Allium sativum*), Garlic plant, Garlic oil and Garlic powder [39].

Administration of 1g of the supplement for 12 weeks significantly reduced the level of resisting, an inflammatory cytokine, thus displaying anti-inflammatory effects [40, 41]. In the last era, the global health community has focused on planning for the prevention and control of a viral pandemic. Proper treatment of infected people with antiviral medication can cure the illness, reduce its severity and also minimize the disease which has arisen due to the outbreak [43].

### 2.4.1 Bioactive Compounds of Garlic

Although garlic has been used since ancient time for its medicinal purposes, the exploration of its active constituents began recently. The Organosulfur compounds of garlic are to be the main bioactive constituents, and are also responsible for its pungent odor [47]. More than thirty sulfur containing compounds belonging to two main chemical classes, L-cysteine sulfoxides and  $\gamma$ -glutamyl-L-cysteine peptides, are presents in garlic. Allicin (S- allyl-L-cysteine sulfoxide) is the most abundant sulfur compound present in fresh and dry garlic (10–30 mg/g). Allinin can quickly convert into allicin (diallyl thiosulfinate) by the action of alliinase enzymes upon chopping, mincing, crushing or chewing of fresh garlic.

Allicin itself is very unstable and can be decomposed in-vitro into other Organosulfur compounds including diallyl sulfide (DAS), diallyl disulfide (garlicin), diallyl trisulfide (allitridin or DATS), andajoene and vinyl-dithiins. Allicin can interact with cellular thiols such as glutathione and L-cysteine in-vivo and form S-allyl-mercapto-glutathione (SAMG) and S-allyl- mercaptocysteine (SAMC), respectively. These compounds may be responsible for the detrimental structural changes of pathogen's proteins [48, 49].

Allicin is the main Organosulfur compounds that was considered one of the principal compounds responsible for antiviral activity, immunomodulatory, anti-inflammatory, antioxidant and other pharmacological properties [43, 44]. The proposed mechanism of their antiviral activity was reported to be the inhibition of the viral cell cycle, enhancing host immune response or reduction of cellular oxidative stress. However, there is no systematic review till date that covers the antiviral activity of garlic and its Organosulfur compounds [45, 46].

## 2.5 Molecular Docking Studies

Molecular docking techniques dock small molecules into the protein binding site. In computational drug designing, when we have to identify a lead compound,

this method is used in order to know many types of binding interaction of the prospective drug with different domains or active sites on the target molecules so that a new drug can be made [47, 48].

## **2.6 Covid Proteins**

### **2.6.1 NSP13**

The helicase protein is also considered as a potential target for the development of anti-HCoV (human coronavirus) agents. It was reported scutellarin and myricetin potently inhibited then sP13 (SARS-CoVhelicaseprotein) invitro by affecting the ATPase activity [49]. The RNA dependent RNA polymerase (RdRp), a key enzyme responsible for both positive and negative strand RNA synthesis, also represents another potential druggable target [43].

### **2.6.2 S Protein**

The main protein that is used in COVID-19 vaccines as a target is S protein. S protein has been categorized into two units such as distal-membrane S1 subunit and a membrane-proximal S2 subunit [43]. The determination of receptor is done by S1 subunit via its receptor-binding domain (RBD). Moreover, the entry of virus is facilitated by membrane fusion that is the function of S2 subunit.

### **2.6.3 N Protein**

The N protein is the most abundant viral protein and is highly immunogenic during CoV infection [39]. It is a major target for antibody responses and also contains T cell epitopes [50]. The inclusion of N protein in CoV vaccines is complicated by balancing immunopathogenesis and viral clearance. Till date, no vaccine for COVID-19 has been reported that is N protein based.

# Chapter 3

## Materials and Methods

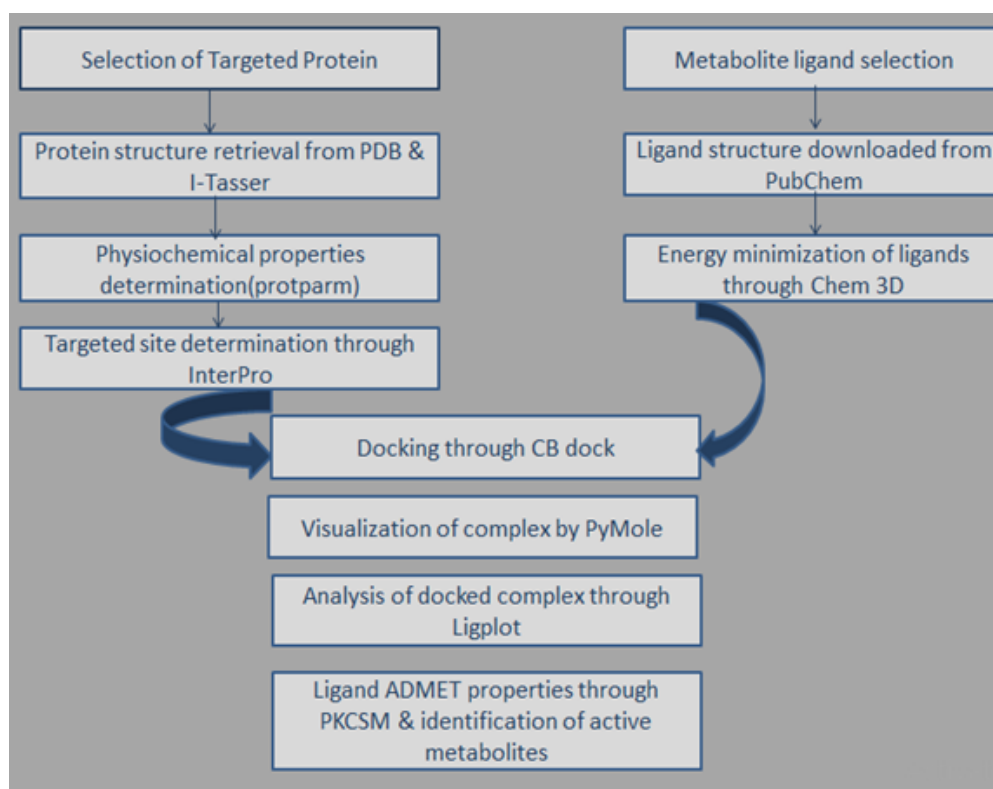


FIGURE 3.1: The flow chart of methodology.

### 3.1 Selection of Disease

The coronavirus disease 2019 (COVID-19) pandemic has drastically affected almost 218 countries while imposing a severe health and economic burden [50]. A

novel coronavirus (SARS-CoV-2) is reported to be the causative agent of this infectious disease with the mode of transmission of COVID-19 [51].

## 3.2 Selection of Protein

One of critical approach is targeting proteins such as nucleoprotein, spike protein which are structural protein and helicases that regulate most of the SARS-CoV-2 RNA metabolism [52].

Structure of SARS-CoV-2 selected protein was retrieved rom Protein Data Bank (PDB ID: 6M2Q) in .pdb format. PDB archive is the only source of information about the 3D structure of large biological molecules [53].

## 3.3 Primary Sequence Retrieval

Primary sequence of target proteins such as nucleoprotein, spike protein which are structural protein and helicases was taken in FASTA format from protein sequence database UniProt (<http://www.uniprot.org>) [53].

## 3.4 Analysis of Physicochemical Properties

This is to determine the function of proteins. ProtParam was used to predict these properties [52]. Physicochemical parameters of SARS-CoV-2 protein including Molecular weight, Number of amino acids, isoelectric point, instability index, grand average of hydropathicity (GRAVY).

Number of negatively charged residues (Asp + Glu), Number of positively charged residues (Arg + Lys), Aliphatic index, and amino acid and atomic composition was investigated by using the ProtParam tool of ExPASy [53].

### 3.5 Identification of Functional Domains

Interpro (<https://www.ebi.ac.uk/interpro/>) was used to detect and predict the functional domain of targeted proteins. Conserved domains are involved in sequence/structure/relationship study [54]. InterPro provides practical analysis of proteins by classifying them into families and predicting domains and active sites.

### 3.6 Active Site Identification

The ligand shows maximum or highest interaction with the protein where the target protein has their active site. Amino acids are highly involved in the formation of complex of ligand to protein. Protein binding pockets were identified by CASTp [55].

### 3.7 Ligand Preparation

The 3-dimensional (3D) structure of ligands was obtained from PubChem. The PubChem is the world's largest collection of freely available chemical information [53]. We can search number of ligands by their names, molecular formula, structure and by other information. If targeted structure is not available PubChem, then can be drawn via ChemDraw by inserting Canonical smileys derived from PubChem [54].

### 3.8 Bioactivity Analysis of Ligands and Toxicity Measurement

Selected ligands from PubChem database should follow the Lipinski rule of five, used to determine chemical compound with pharmacological or biological activity

has chemical properties and physical properties. The potential success of a compound depends on its ADMET properties. PkCSM (<https://omictools.com/pkcsm-tool>) is an online tool that helps to find the ADMET properties [58].

### 3.9 Molecular Docking Process

The purpose of molecular docking is to find the best conformational interaction between target proteins and compounds. The two essential requirements for docking are the target protein and the candidate ligand. Molecular docking of protein and ligands was done through Cavity-detection guided Blind Docking (CB-Dock) [59].

### 3.10 Visualization of Ligand/Protein via PyMol

Docked complex of ligand and protein was visualized by PyMol. This is capable of editing molecules, ray tracing and making movies [51]. Docking poses generated via CB-Dock were visualized and saved as a molecule in .pdb form in one file for further analysis [52].

### 3.11 Analysis of Docked Complex via LigPlot

Analysis of docked complex was done by LigPlot, that generates automatically schematic diagrams of protein-ligand interactions for given PDB file. These interactions are modified by hydrogen bonds and through hydrophobic contact [59].

### 3.12 Ligand ADMET Properties

The main aim of preclinical ADMET is to choose strong candidates by eliminating weak drug candidates in the early stages of drug development. Optimization of

the ADME (Absorption, Distribution, Metabolism, and Excretion) properties of the drug molecule was done by using PkCSM [60].

### **3.13 Active Inhibitor Identification**

After a detailed analysis of protein and ligand interactions, docking scores and toxicity studies, the most active inhibitor was identified. The selected compound is our lead compound [61].

### **3.14 FDA Approved Drug-Proposed Antioxidant Agent Comparison**

The comparison between selected antioxidant drugs and proposed antioxidant agents is done by comparing docking results, physiochemical properties and ADMET properties. The comparison is made easy by Byju's Greater Than Calculator" online learning app ([byjus.com/greater than calculator/](https://byjus.com/greater-than-calculator/)) which helps in identifying smaller and greater values [62].



# Chapter 4

## Results and Discussion

### 4.1 Target Proteins from UniProt

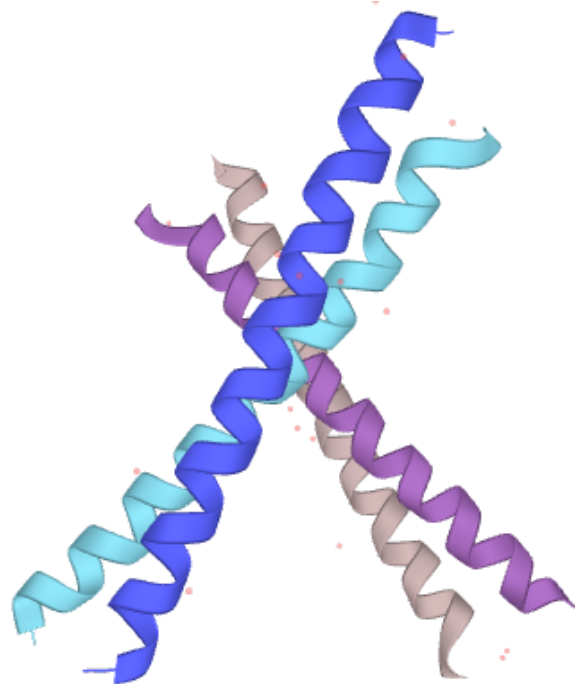
#### 4.1.1 Primary Sequence Retrieval

Primary sequence of target protein (nucleoprotein) was taken in FASTA format from Uniprot database (<http://www.uniprot.org>) under accession number P04179, P07203, P04040 with 222, 203, and 527 residues length [62].



```
>MSDNGPQNRNAPRITFGGSPDSTGSNQNGERSGARSKQRRPQGLPNNTASWFTALTQHGKEDLKFRGQGVPIN
TNSSPDDQIGYYRRARRIRGGDGKMKDLSRWYFYLLGTGPEAGLPYGANKDGIWVATEGALNTPKDHIGTRNPAN
NAAIVLQLPQGTTLPKGFYAEGSRGGSQASSRSSRSRNSRNSTPGSSRGTS ParmMAGNGGDAALALLLDRLNQLES
KMSGKGGQQGQTVTKKSAEASKKPRQKRTATKAYNVTQAFGRRGPEQTQGNFGDQELIRQGTDYKHWPQIAQF
APSASAFFGMSRIGMEVTPSGTWLTYTGAIKLDDKDPNFKDQVILLNKHIDAYKTFPPTPEPKDKKKKADETQALPQRQ
KKQQTVTLPAADLDDFSKQLQQSMSSADSTQA
```

FIGURE 4.1: Fasta sequence and structure of nucleoprotein (target protein) [62].



```
>MFVFLVLLPLVSSQCVNLTRTQLPPAYTNSFTRGVYYPDKVFRSSVLHSTQDLFLPFFSNVTWFHAIHVSGTNGTKRF
DNPVLPFNDGVYFASTEKSNIRGWIFGTTLDSTQSLIVNATNVVIKVEFCNDPFLGVYHKNKSWMESEFR
VYSSANNCTFEYVSPFLMDLEGKQGNFKNREFVFNIDGYFKIYKHTPINLVRDLPQGFSALEPLVDLPIGINITRFQT
LLALHRSYLTPGDSSSGWTAGAAAYVGYLQPRFTLLKYNENGTITDAVDCALDPLSETKCTLSFTVEKGIYQTSNFRVQ
PTESIVRFPNITNLCPFGEVFNATRFASVYAWNRKRISNCVADYSVLYNSASFSTFKCYGVSPTKLNDLCFTNVYADSFVIR
GDEVRQIAPGQTGKIADYNYKLPDDFTGCVIAWNSNLDKSKVGGNYNYLRLFRKSNLKPFRDISTEIQAGSTPCNG
VEGFNCYFPLQSYGFQPTNGVGYQPYRVVLSFELLHAPATVCGPKKSTNLVKNKCVNFNGLTGTGVLTESNKKFLP
FQQFGRDIADTTDAVRDPQTEILDITPCSFGGVSVITPGTNTSNQVAVLYQDVNCTEVPVAIHADQLTPTWRVYSTGS
NVFQTRAGCLIGAEHVNSYECDIPIGAGICASYQTQNSPRRARSVASQSIAYTMSLGAENSVAYSNSIAIPTNFTISV
TTEILPVSMTKTSVDCTMYICGDSTECNLLLQYGSFCTQLNRALTGIAVEQDKNTQEVFAQVKQIYKTPPIKDFGGFNFS
QILPDPSPKRSFIEDLLFNKVTLDAGFIKQYGDCLGDIARDLCAQKFNGLTVLPLLTDemiaQYTSALLAGTITSG
WTFGAGAALQIPFAMQMAYRFNGIGVTVQNVLYENQKLIANQFNSAIGKIQDLSSTASALGKLDQDVVNQNAQALNTL
VKQLSSNFGAISSVLNDILSRDKVEAEVQIDRLITGRLLQSLQTYVTQQLIRAAEIRASANLAATKMSECVLGQSKRVDFC
GKGYHLMSFPQSAPHGVVFLHVTYVPAQEKNFHTTAPAICHGKAHFPREGVFSNGTHWFVTQRNFYEPQIITDNTF
VSGNCDVVIGVNTVYDPLQPELDSFKEELDKYFKNHTSPDVLGDISGINASVNIQKEIDRLNEVAKNLNESLIDLQE
LGKYEQYIKWPWYIWLGFIAGLIAIVMVTIMLCCMTSCCCLKGCCSCGSCCKFDEDDSEPVKGVKLHYT
```

FIGURE 4.2: Structure and Fasta Sequence of Spike Protein (Target Protein) [62].



```
>MELRSYQWEVIMPALEGKNIIVLPTGAGKTRAAAYVAKRHLETVDGAKVVVLVNRVHLVTQHGEEFRRMLDGRWT
VTTLSGDMGPRAGFGHLARCHDLLICTAELLQMALTSPEEEHVVELTVFSLIVVDECHHTHKDVTYNVIMSQYLELKLQR
AQPLPQVLGLTASPGTGGASKLDGAINHVLQLCANLDTWCIMSPQNCCPQLQEHSQQPCKQYNLCHRRSQDPFGDLL
KKLMDQIHDHLEMPELSRKFGTQMYEQVVKLSEAAALAGLQEQRVYALHLRRYNDALLIHDTVRAVDALAALQDFY
HREHVTKTQILCAERRLLALFDDRKNELAHLATHGPNPKLEMLEKILQRQFSSNSPRGIIFTRTRQSAHSLLLWLQQQ
QGLQTVDIRAQLLIGAGNSSQSTHMTQRDQQEVIQKFQDGTLLNLLVATSVAEEGLDIPHNCNVVRYGLLTNEISMVQA
RGRARADQSVYAFVATEGSRELKRELINEALETLMQAVAAVQKMDQAEYQAKIRDLLQQAALTKRAAQAAQRENQR
QQFPVEHVQLLCINCMVAVGHGSDLRKVEGTHHVNVNPNFNSNYNVSRDPVVINKVKFDWKPGGVISCRNCGEWW
GLQMIYKSVKLPVLKVRSMILLETPQGRIQAKKWSRVPFSPDFDLQHCAENLSDLSLD
```

FIGURE 4.3: Structure and Fasta Sequence of Helicases (Target Protein) [62].

### 4.1.2 3D Structure Predictions of Protein

3D Structures of targeted proteins (nsp Protein, N Protein, S Protein) were downloaded from RCSB PDB in PDB format. Protein Data Bank (PDB) is a three-dimensional database of complex molecules of living organisms, such as proteins and nucleic acids. [63].

I-TASSER (Iterative threading ASSEMBly Refinement) server has been widely used to predict structure and function of proteins in biological and biomedical

investigations. I-TASSER predicts regions of secondary structure like alpha helix, beta sheet and coils from the amino acid sequence [64]. I-TASSER server team mails complete results of job id with five models and on the basis of c-score best 3D structural model can be easily selected. The selected target protein is shown in Figure 4.4.



FIGURE 4.4: Structure of SARS-CoV-2 3CL protease (3CL pro) protein [63].

SARS-CoV-2 is the virus which is responsible in order to cause covid-19 and uptill now there is no proper treatment for this pandemic which has affected all the world. In order to know about the virus it is compulsory to get informnation

about the structure of the involved virus. So, this structure shown above can be understood in better way. So, 3CL protease comes from class of highly conserved viruses and it is now the target of antiviral drugs which are broadspectrum in order to kill the virus as it is site of replication of virus [65].

In the early studies on the SARS-CoV-2 models Mpro shows close relation to main proteases named coronaviral in means of structure. The 99% of the aminoacid structure is common of batCoV, RaTG13 Mpro and 97% similar to the SARS-CoV Mpro [66].

## 4.2 Functional Domain Identification of Proteins

Interpro is a resource for functional analysis of protein sequences. Conserved domains are involved in sequence/structure/relationship. Proteins can have more than one functional domain that perform different functions.

Functional domain is the active part of a protein that is involved in interactions of proteins with other substances [67]. These functional domains and families of protein were shown in the Figure 4.5. These functional domains help in performing different important functions.

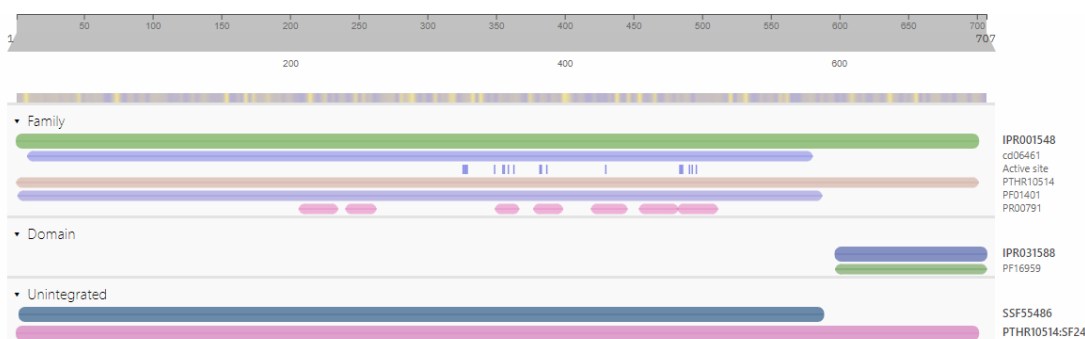


FIGURE 4.5: Conserved domains of target protein [67].

In the Figure 4.6 given below shows functional domains and pockets present in red color along the structure of protein. Moreover, the Table 4.1 shows the area and volume of these pockets which were obtained by using CASTp software [68].

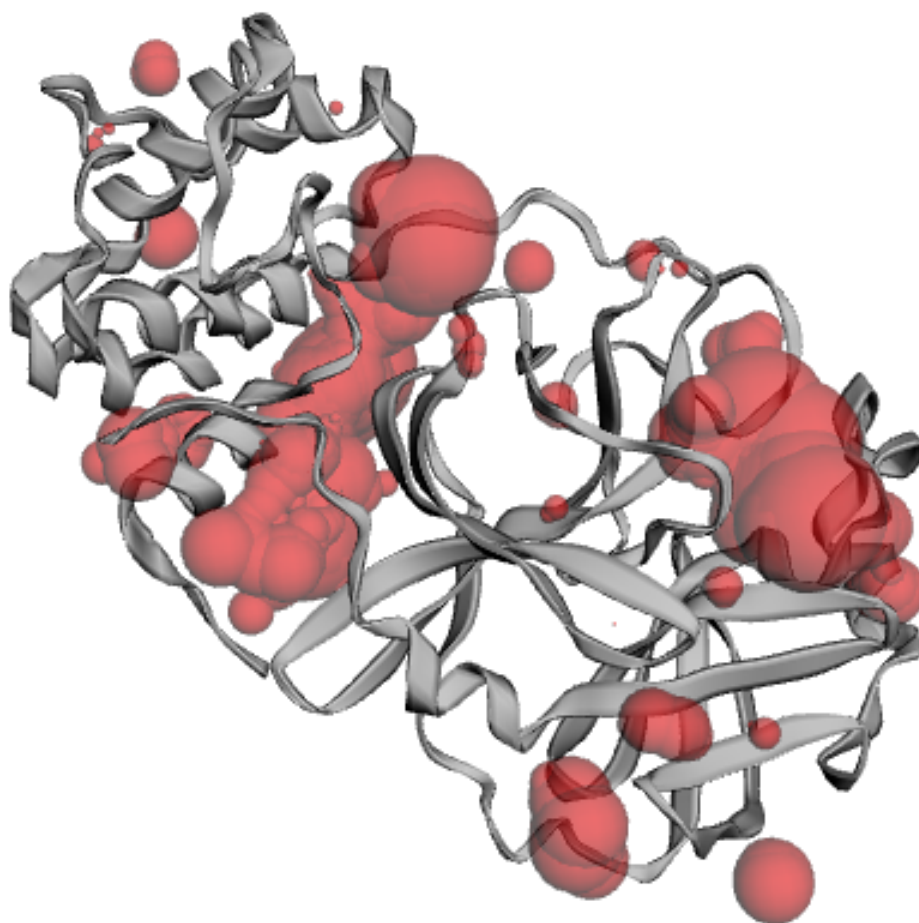


FIGURE 4.6: Functional domains of target protein [68].

TABLE 4.1: Area and volume of the obtained pockets by CASTp [68]

Pocket ID	Area (SA)	Volume (SA)
1	284.664	292.690
2	273.913	214.993
3	53.189	59.074
4	104.306	30.390
5	40.514	25.655
6	27.458	7.991
7	20.634	7.083
8	13.671	4.642
9	6.817	3.399

---

10	16.544	3.174
11	10.896	2.007
12	10.676	1.878
13	6.664	1.663
14	6.528	0.747
15	4.217	0.743
16	6.818	0.470
17	4.637	0.424
18	4.031	0.356
19	1.004	0.163
20	1.770	0.100
21	0.993	0.038
22	0.744	0.020
23	0.265	0.006
24	0.103	0.002
25	0.071	0.001
26	0.046	0.000
27	0.001	0.000
28	0.022	0.000
29	0.000	0.000
30	0.013	0.000
31	0.042	0.000

---

### 4.2.1 Ligand Selection

Protein data bank contains a large amount of protein ligand complex, especially for the protein target. Therefore, the selection of ligands is based on the best resolution of the structure, the chemical class of the co-crystal ligand bound to the protein structure and the best binding unity. Conformational selection is a process in which ligand selectively binds to one of these conformers, strengthening

it and increasing its population with respect to the total population of the protein is ultimately resulting in the final observed complex [68]. Ligands (compounds of the selected plant) were searched out from Pub Chem, which is the world's largest freely accessible chemical information database. Their 3-D structures were downloaded from PubChem in SDF format. Selected compounds were representing all the classes of compounds like phenols, terpenoids, essential oils, and steroids, etc [69].

After selection of ligands, energy minimization of ligands was carried out by chem pro software (chem 3D v12.0.2). This was a mandatory step in the preparation of ligands for docking because unstable ligands will show unreliable vina scores in docking results. Bioactive compounds of *Allium sativum* were selected as ligands for the present study [70].

The 3D structures and information of selected ligands that are 3-(Allylsulphinyl)-L-alanine, Alicin, Diallyl sulfide, Diallyl disulfide, Diallyl trisulfide, Glutathione, L-Cysteine, S-allyl-mercapto-glutathione, Thiocysteine, gamma-glutamyl-Lcysteine, gamma glutamyl allyl cysteine, Quercetin, myricetin Kaempferol, Fructan, Lauric acid, Linoleic acid, Allixin, Ajoene, diazinon, levamisole, caffeic acid, Ethyl linoleate, Scutellarein, and S-allylcysteine methylester are downloaded from PubChem. This all obtained information is noted in the table 1 (ref to Appendix A) This database (<https://pubchem.ncbi.nlm.nih.gov>) is a public database used to collect information and data on different chemical compounds and their activities [71].

### 4.3 Molecular Docking

It is technique which is used to estimate the strength of a bond between a ligand and a target protein through a special scoring function and to estimate the correct structure of the ligand present in the binding site of the target. The 3D structure of the target proteins and the ligands is taken as the input for docking [81]. After preparing proteins and ligands ready for docking, docking were performed by CB dock which is a well trusted online blind auto docking tool. The results and time



required for docking is depend upon structures of receptors, ligands, requirements, and net speed. It may take several hours for a single result so patience was shown while doing docking. CB dock gave us possible possess and receptor models and among these possess best one was selected by observing certain properties like vena score and size of cavity etc [82].

Molecular docking without having information of binding sites is performed by using a user friendly blind docking web server called as CB Dock, which predicts and estimate a binding site for protein and calculate centers and sizes with a novel rotation cavity detection method and perform docking with the popular docking program known as Auto dock Vina [83]. So, the obtained data is given in the Table 4.2 which shows minimum and maximum energy, cavity size, binding score and grid map of ligands.

TABLE 4.2: Results of CB dock [82, 83].

Sr. No	Ligand	Binding Score	Cavity size	Grid Map	Min-energy (Kcl/mol)	Max-energy (Kcl/mol)
1	3-(Allylsulphinyl)-L-Alanine	-4.8	1385	26	0	1.60E+00
2	Allicin	-3.2	1385	26	0	1.60E+00
3	Diallyl Sulfide	-3.1	1385	26	0	1.60E+00
4	Diallyl Disulfide	-3.5	1385	26	0	1.60E+00
5	Diallyl Trisulfide	-5.5	277	21	0	1.60E+00
6	Glutathione	-5.8	277	21	0	1.60E+00
7	L-Cysteine	-3.7	1385	26	0	1.60E+00
8	S-Allyl-Mercapto-Glutathione	-6	277	22	0	1.60E+00
9	Thiocysteine	-3.8	1385	21	0	1.60E+00
10	Gamma-Glutamyl-L-Cysteine	-7.2	1385	24	0	1.60E+00
11	Gamma-Glutamyl-S-Allylcysteine	-5.4	1385	21	0	1.60E+00

---

12	Kaempferol	-7.4	1385	26	0	1.60E+00
13	Quercetin	-7.6	1385	21	0	1.60E+00
14	Myricetin	-7.8	1385	21	0	1.60E+00
15	Fructan	-7.1	1385	21	0	1.60E+00
16	Lauric Acid	-5.2	1385	22	0	1.60E+00
17	Linoleic Acid	-5.7	1385	30	0	1.60E+00
18	Allixin	-5.8	1385	26	0	1.60E+00
19	Ajoene	-4.7	1385	22	0	1.60E+00
20	Ethyl Linoleate	-5.8	1385	31	0	1.60E+00
21	Diazinon	-5.7	1385	26	0	1.60E+00
22	Levamisole	-5.7	1385	26	0	1.60E+00
23	Scutellarein	-7.6	1385	21	0	1.60E+00
24	S-allylcysteine methylester	-5.3	1385	21	0	1.60E+00
25	Caffeic acid	-5.8	1385	26	0	1.60E+00

---

## 4.4 Interaction of Ligands and Target Protein

Molecular docking without having information of binding sites is performed by using a user friendly blind docking web server called as CB Dock. The docking analysis was performed by using LigPlot+ (version v.1.4.5) and PyMol Edu (v1.7.4.5). Interactions of ligands and target proteins are predicted by using Ligplot plus (version v.1.4.5).

The graphical system of LigPlot+ automatically generates multiple 2D diagrams of interactions from 3D coordinates [71]. The 2D diagrams of the best binding score ligands with respective proteins are obtained from ligplot plus shown in Figures 4.7 to 4.32 while their hydrogen bonds and hydrophobic interactions are listed in Table 4.3. Figure 4.7 shows the interaction of ajoene. As evident from 2D diagram ligand show only hydrophobic interactions with protein.

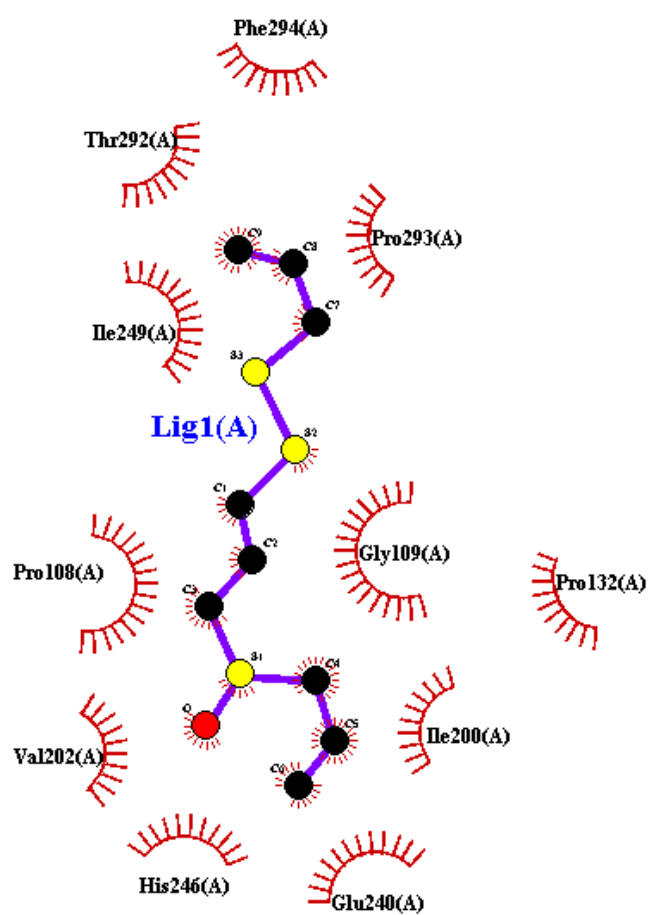


FIGURE 4.7: Interactions of Ajoen with target protein obtained By Ligplot.

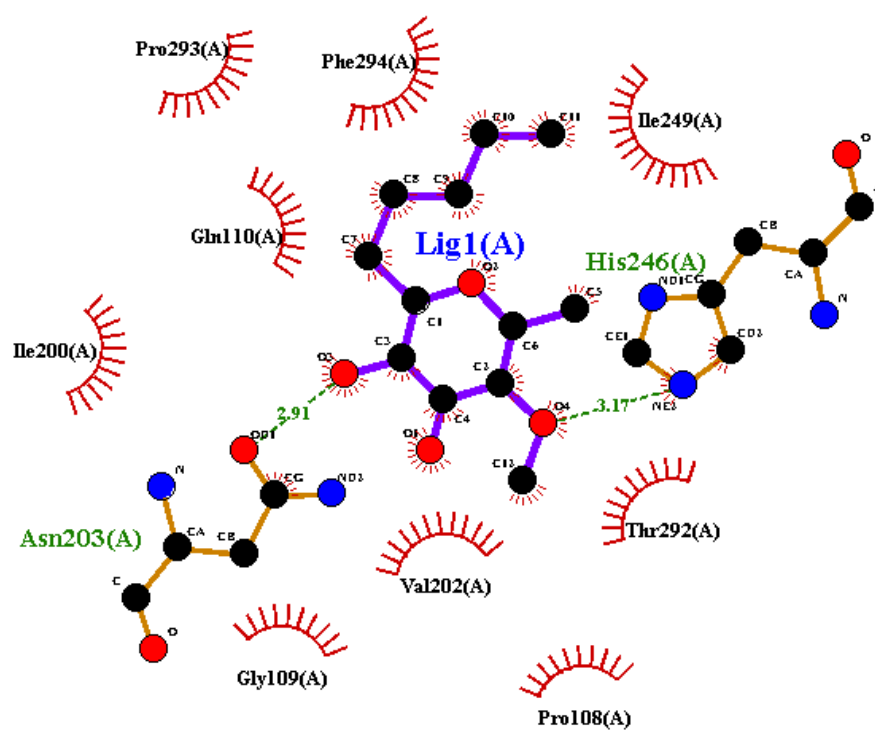


FIGURE 4.8: Interactions of Allixin with target protein obtained By Ligplot.

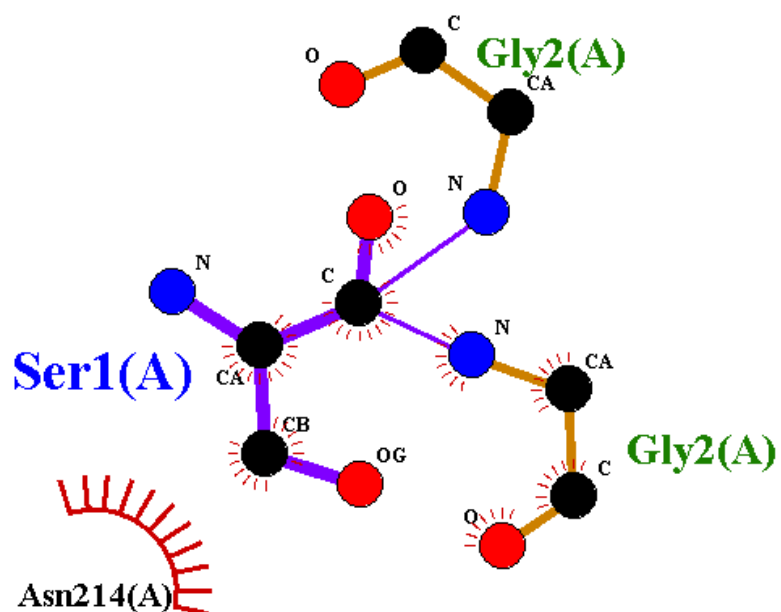


FIGURE 4.9: Interactions of diallyl disulfide with target protein obtained By Ligplot.

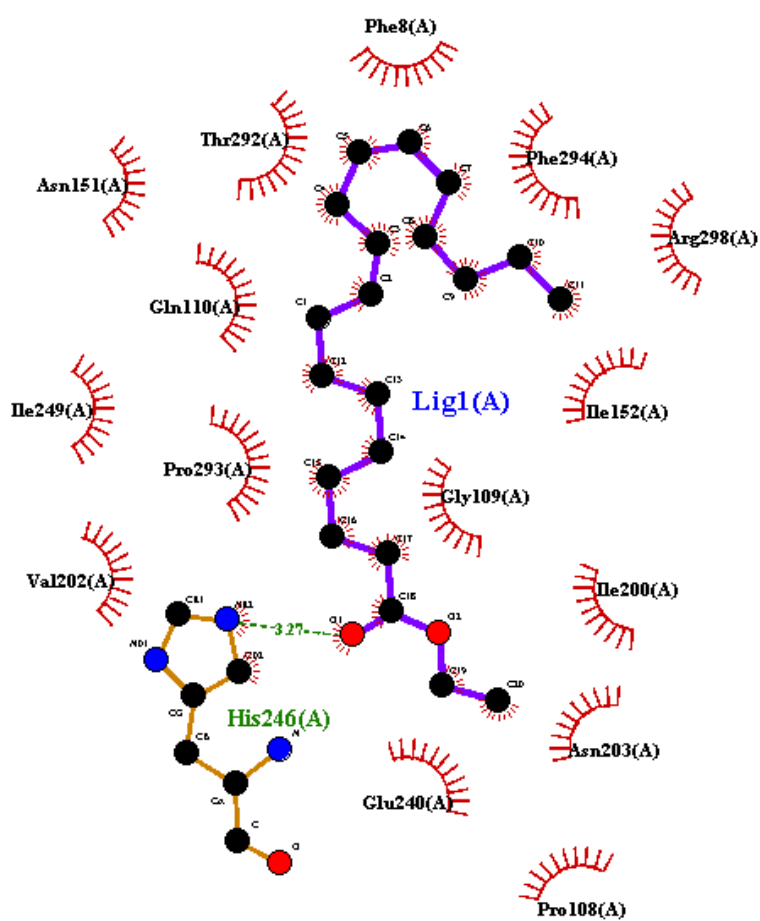


FIGURE 4.10: Interactions of linoleate with target protein obtained By Ligplot.

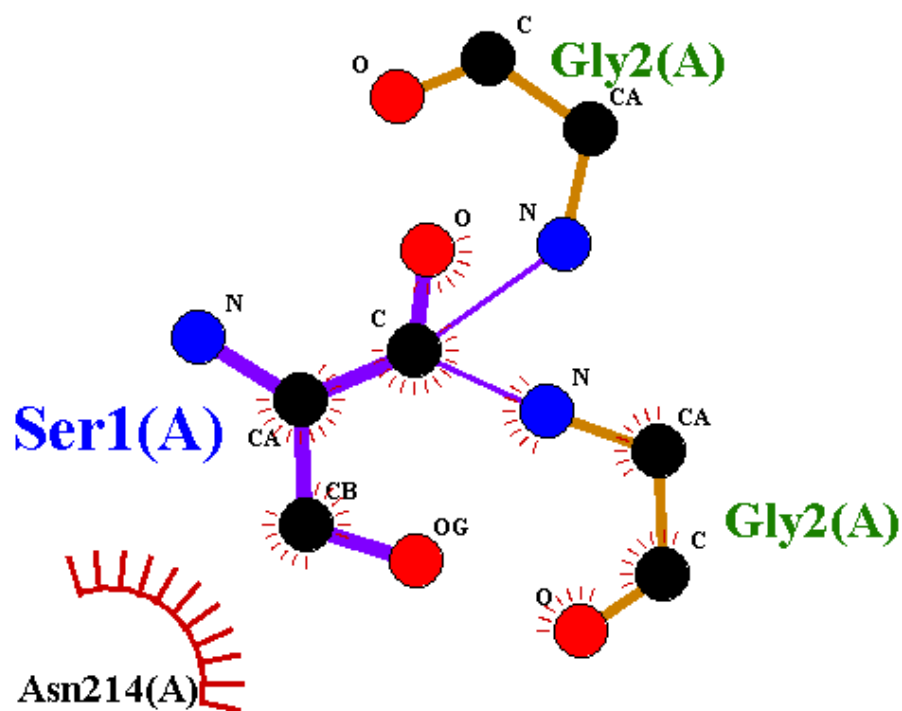


FIGURE 4.11: Interactions of Gamma-Glutamyl-S-Allylcysteine with target protein obtained By Ligplot.

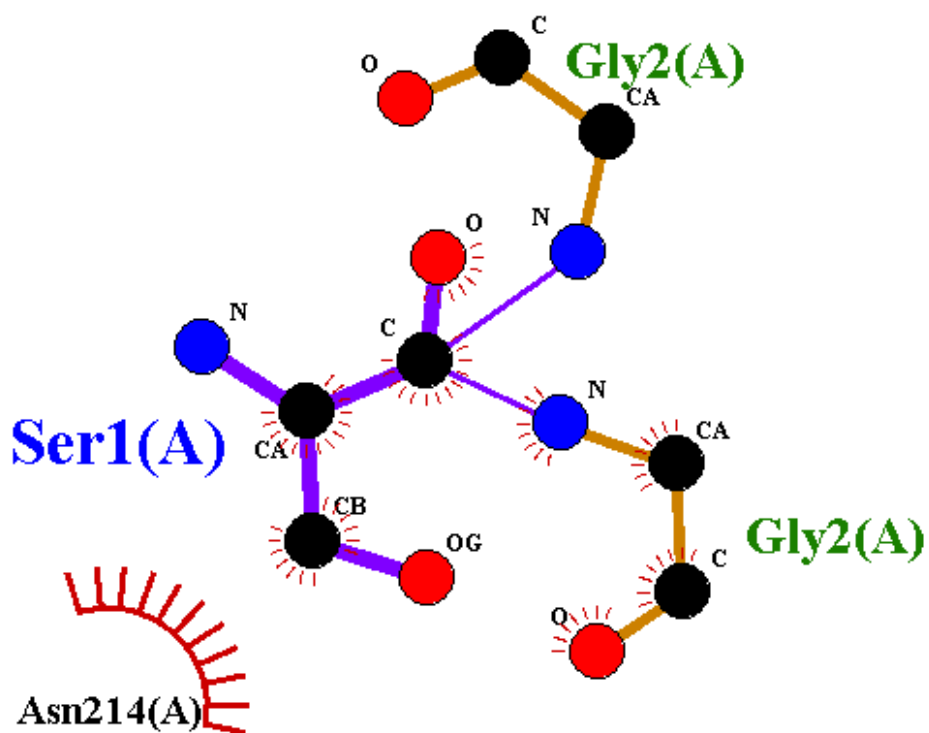


FIGURE 4.12: Interactions of lauric acid with target protein obtained by ligplot.

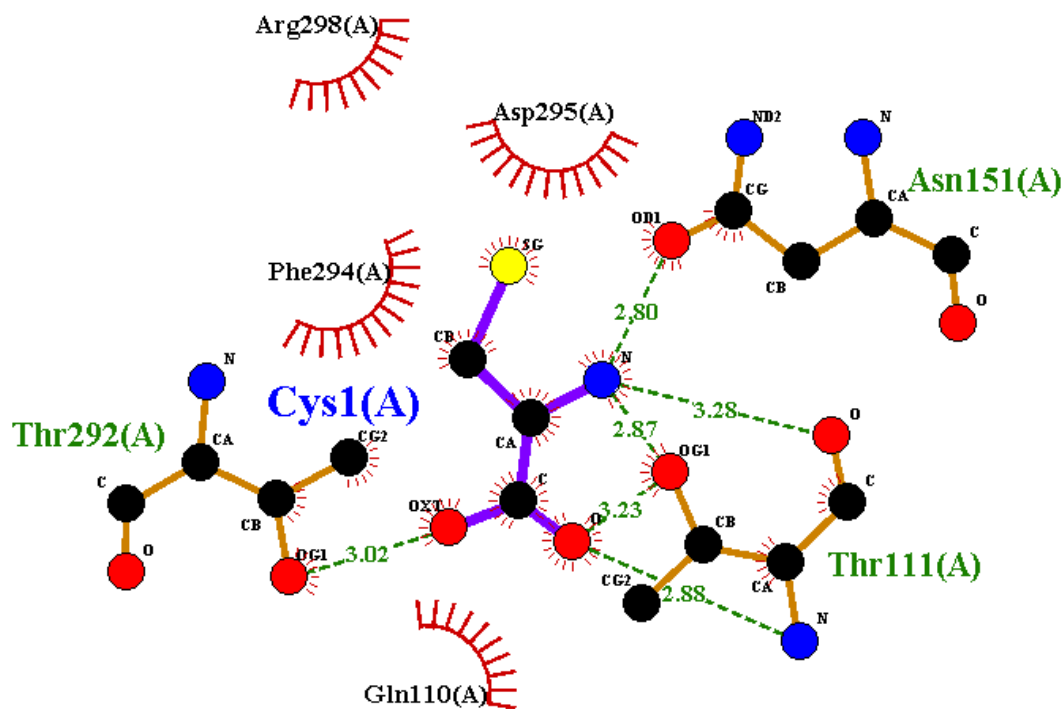


FIGURE 4.13: Interactions of l-cystein with target protein obtained by ligplot.

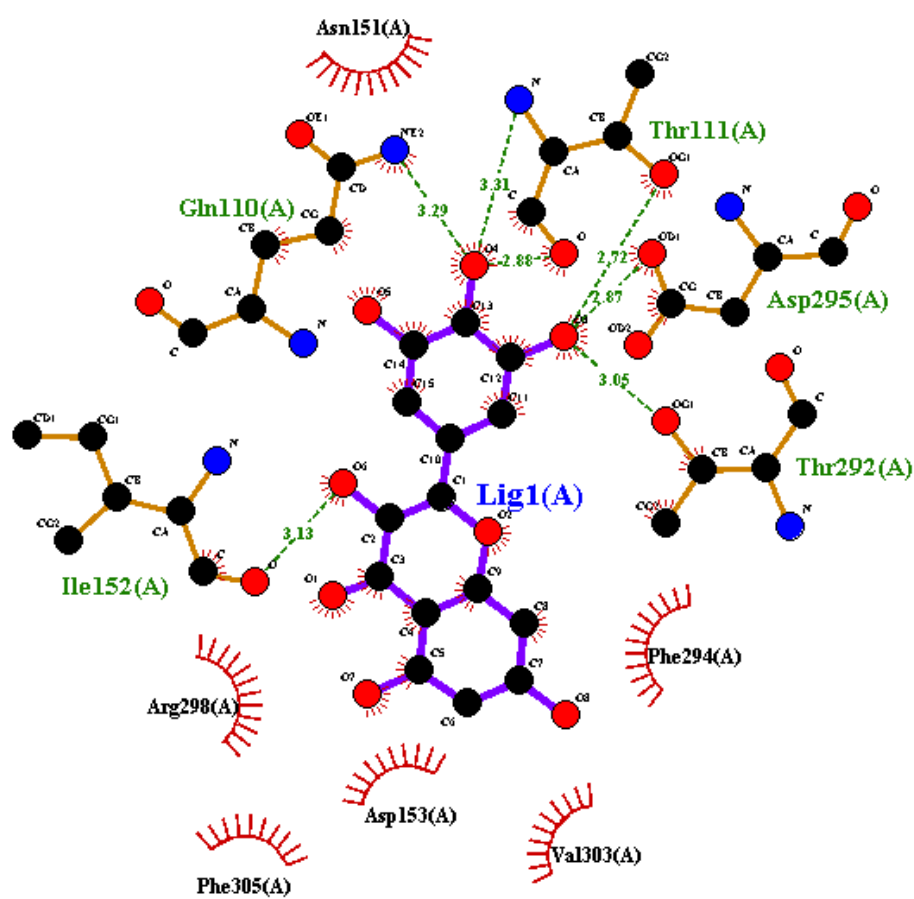


FIGURE 4.14: Interactions of Myrecetin with target protein obtained by ligplot.

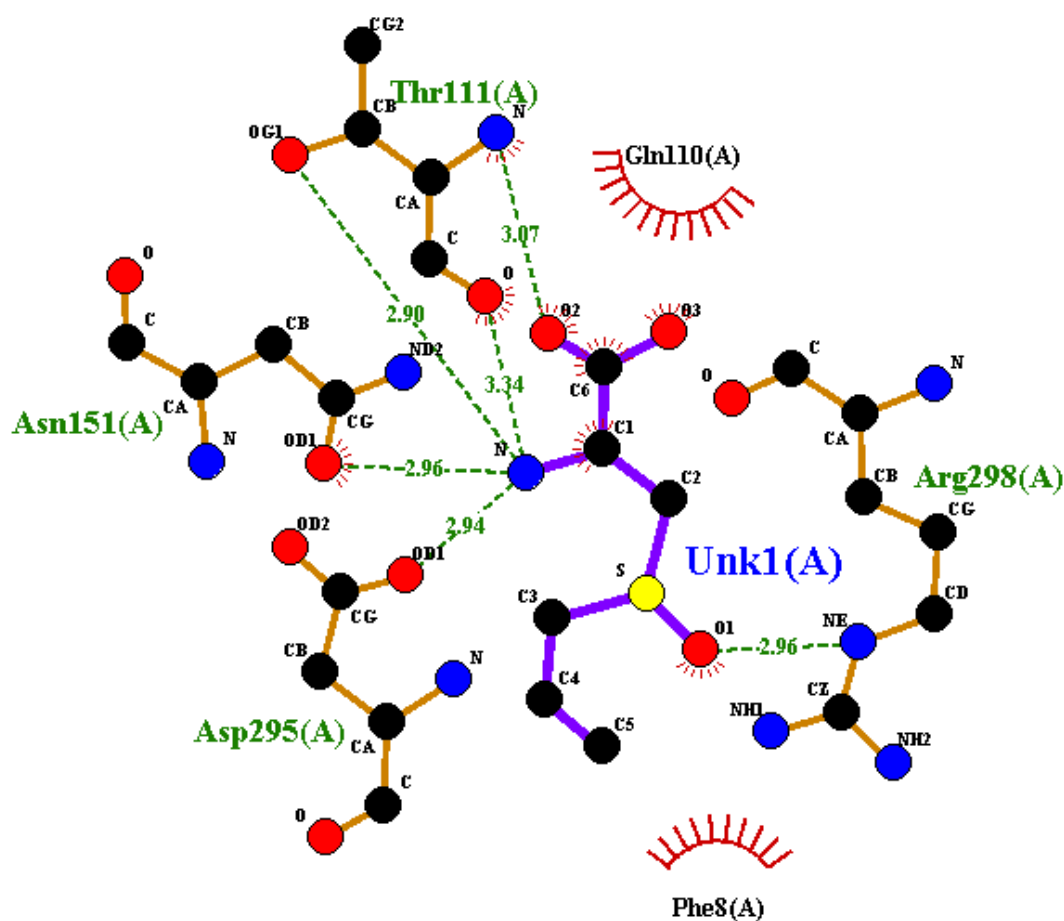


FIGURE 4.15: Interactions of 3-(Allylsulphonyl)-L-Alanine with target protein obtained by ligplot.

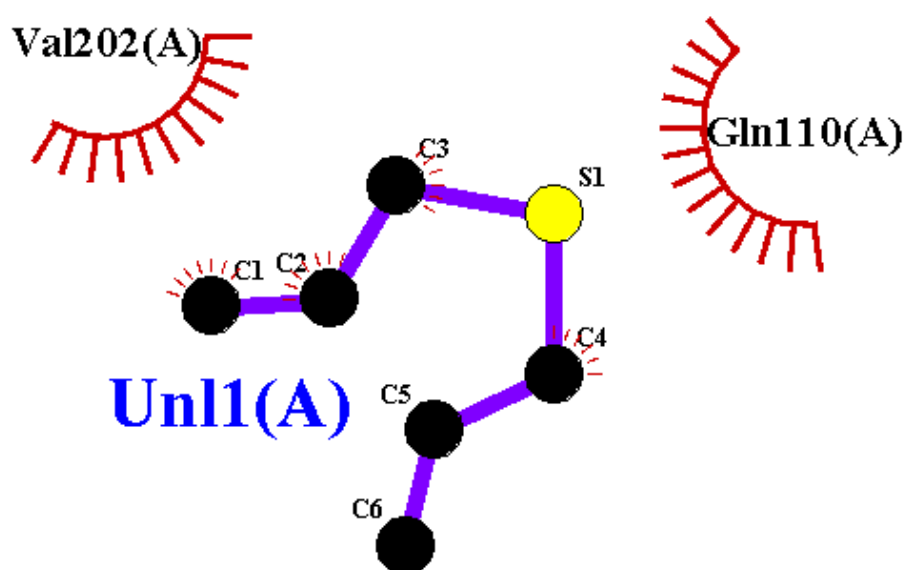


FIGURE 4.16: Interactions of allicin with target protein obtained by ligplot.

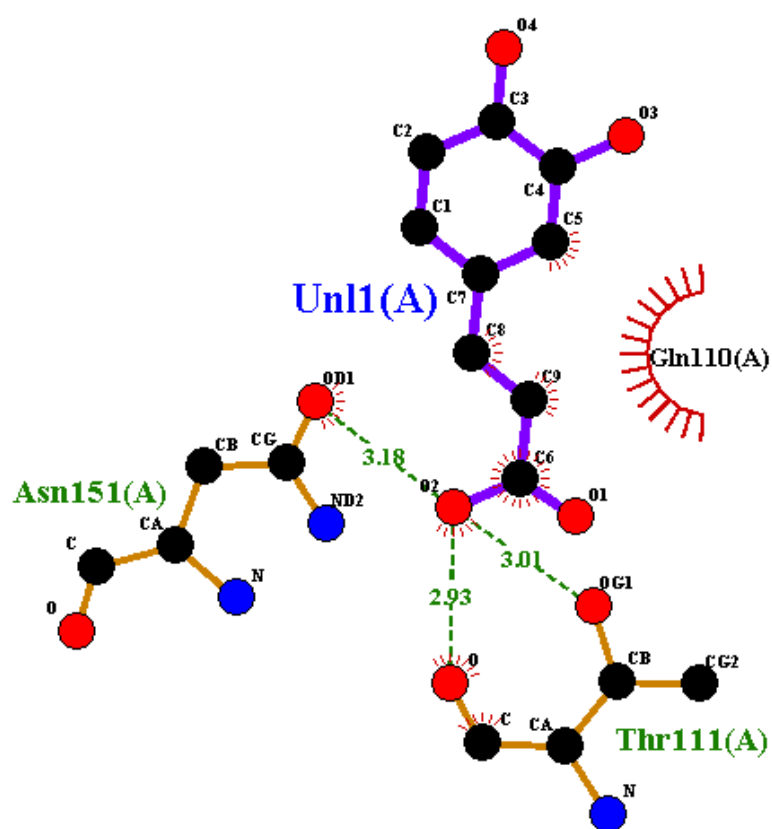


FIGURE 4.17: Interactions of caffeic acid with target protein obtained by ligplot.

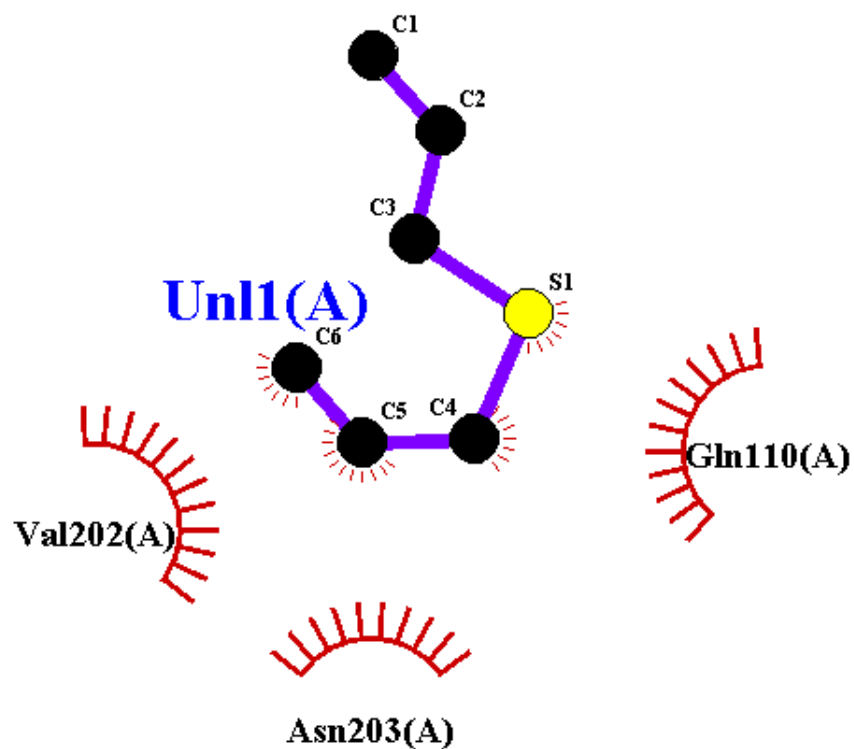


FIGURE 4.18: Interactions diallyl sulfide with target protein obtained by ligplot.





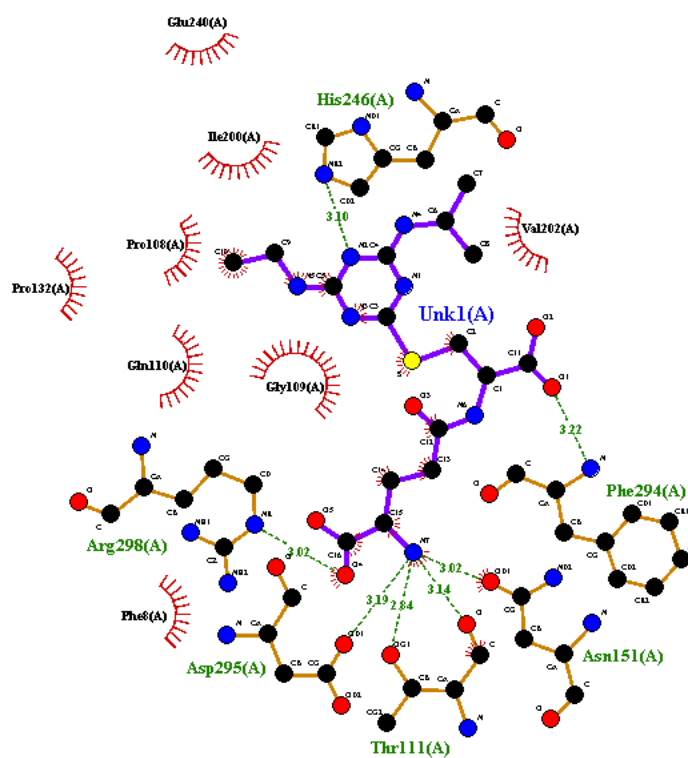


FIGURE 4.21: Interactions of Gamma-Glutamyl-L-Cysteine with target protein obtained by ligplot.

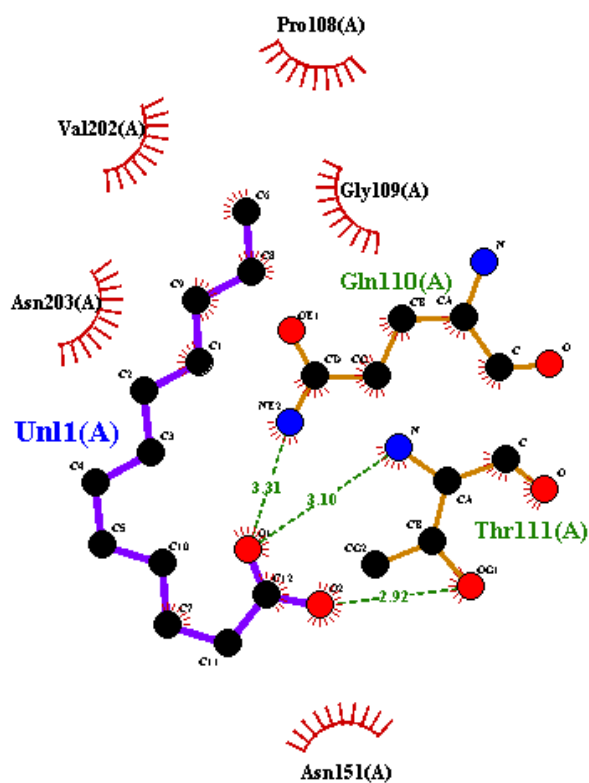


FIGURE 4.22: Interactions of Lauric acid with target protein d obtained by ligplot.

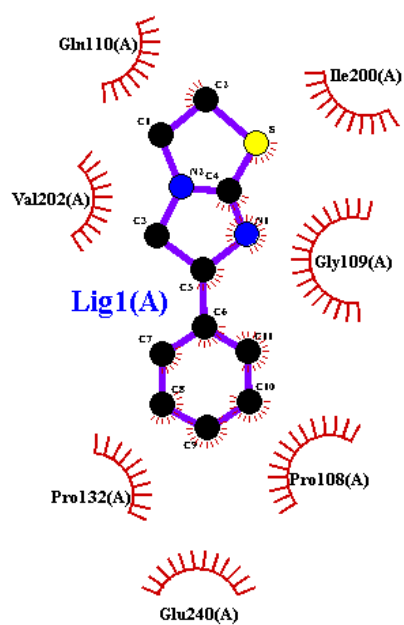


FIGURE 4.23: Interactions of Levamisole with target protein obtained by ligplot.

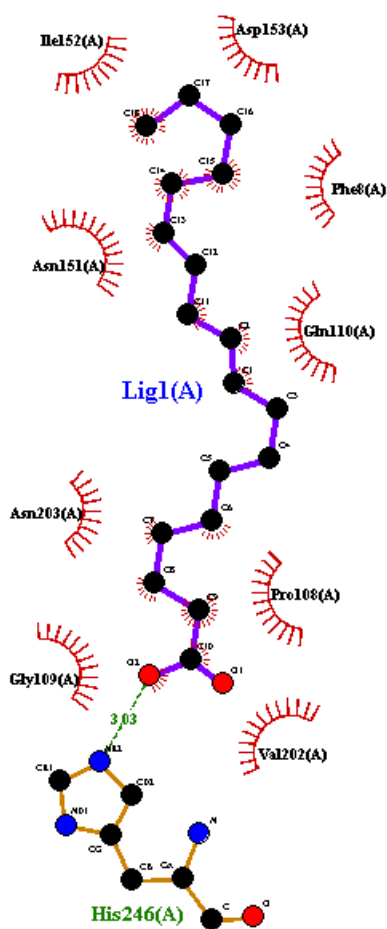


FIGURE 4.24: Interactions of Linoleic acid with target protein obtained by ligplot.

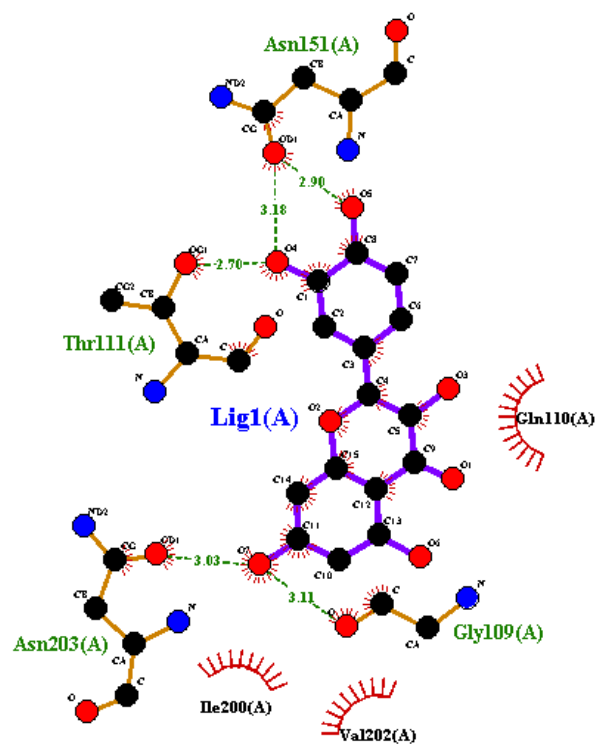


FIGURE 4.25: Interactions of quercetin with target protein obtained by ligplot.

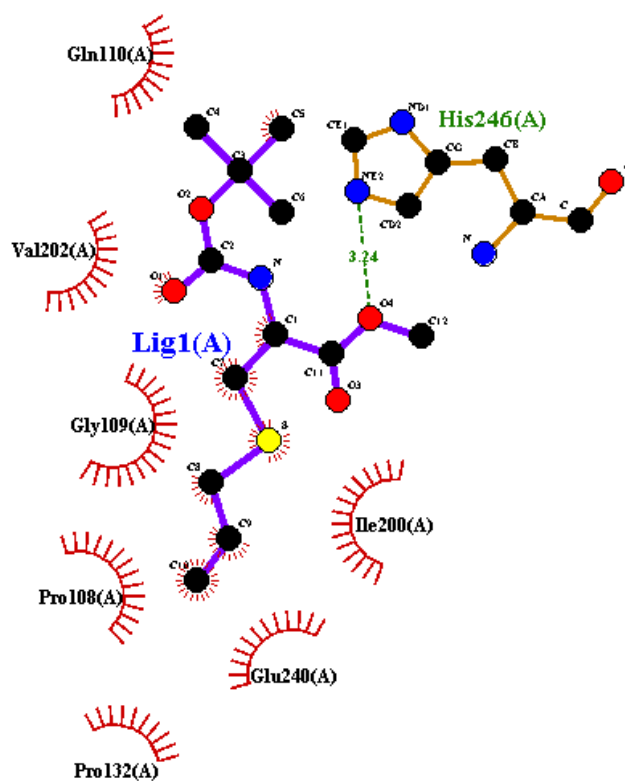


FIGURE 4.26: Interactions of S-allylcysteine methylester with target protein obtained by ligplot.

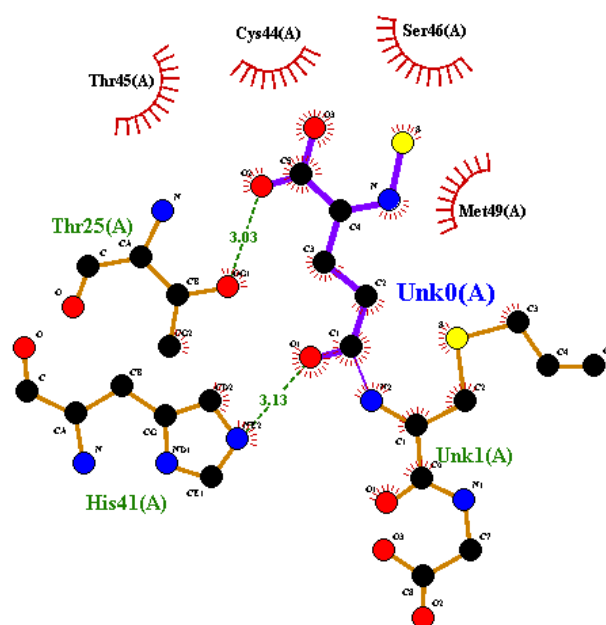


FIGURE 4.27: Interactions of S-allyl-mercapto-glutathione with target protein obtained by ligplot.

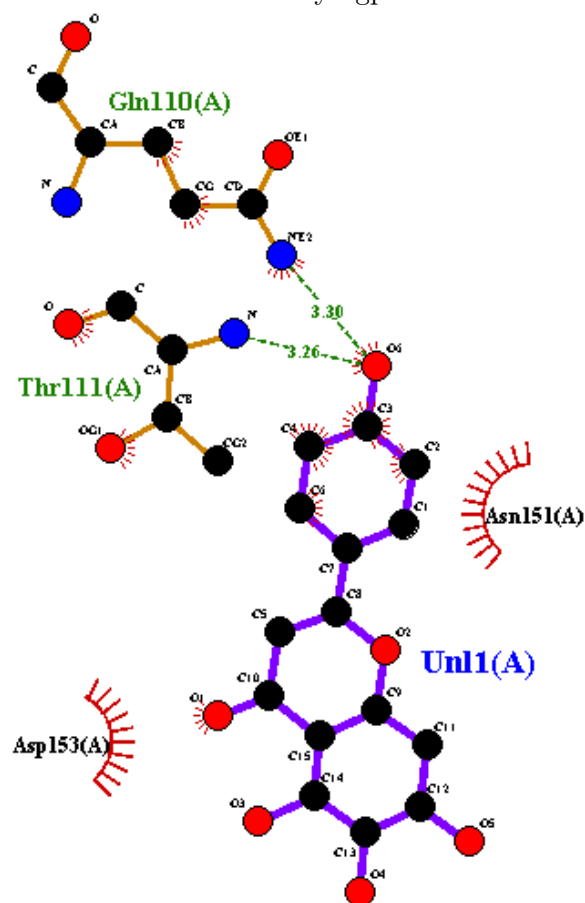


FIGURE 4.28: Interactions of scutellarein with target protein obtained by ligplot.

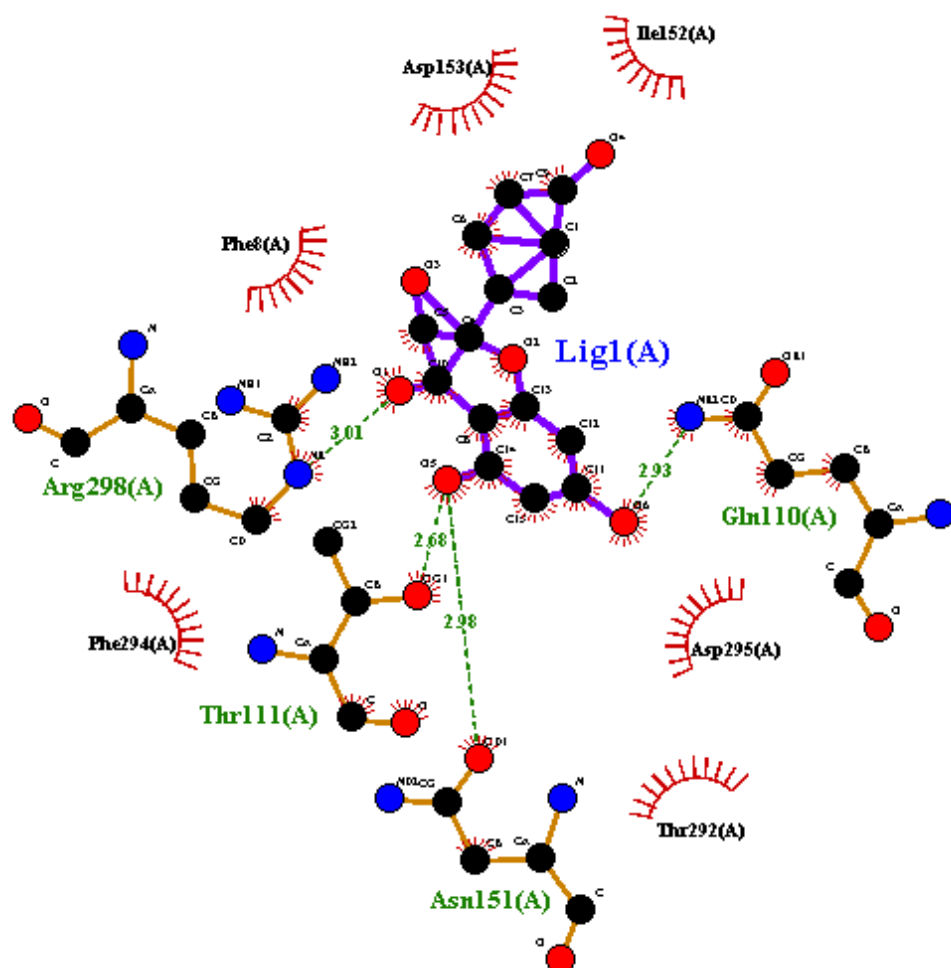


FIGURE 4.29: Interactions of glutathione with target protein obtained by ligplot.

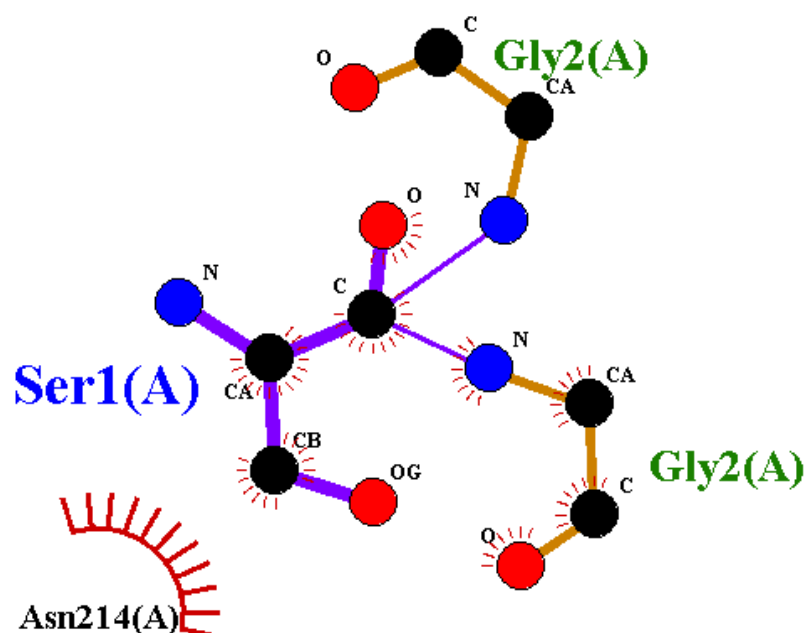


FIGURE 4.30: Interactions of thiocysteine with target protein obtained by ligplot.

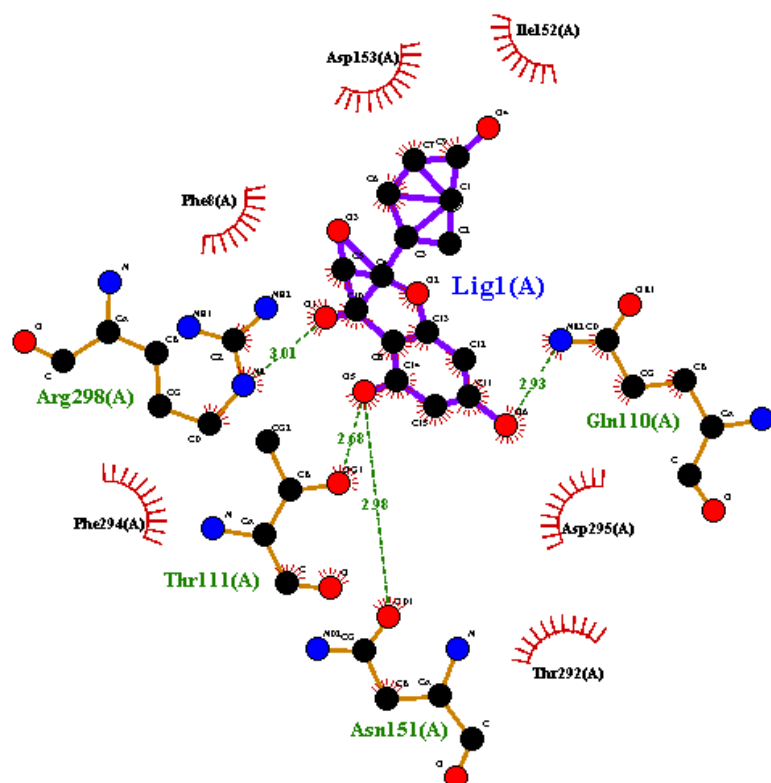


FIGURE 4.31: Interactions of kaomferol with target protein obtained by ligplot.

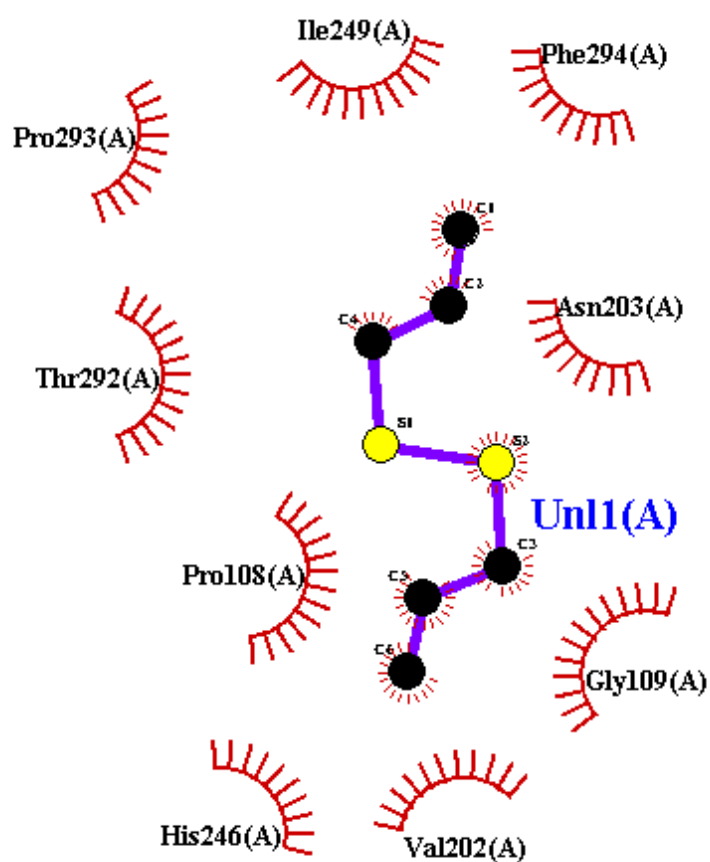


FIGURE 4.32: Interactions of diallyl trisulfide with target protein obtained by ligplot.

The results obtained by ligplot were presented in the form of Table 2 (refer to Appendix B) where interactions of ligands with protein, hydrogen bonds present, their distance, specific amino acids and hydrophobic bonding is presented. Ligand consists of 10 carbons and shows hydrophobic interactions with Pro132, Pro293, Pro108, Thr292, Gly109, Ile200, Ile249, Glu240, His246, Val202 and Phe294 residues as evident also from Table 2 (refer to Appendix B) Allicin, Diallyl Sulfide, Diallyl Disulfide, Diallyl Trisulfide, levamisole, diazinon, thiocysteine, gamma-glutamyl-S-allyl cysteine and ajoene ligands are without hydrogen bonds as it is evident from their 2D structures they are mostly without active oxygen atoms. S-allyl cysteine methyl ester, ethyl linoleate, linoleic acid have one hydrogen bond. S-allyl-mercapto-glutathione, caffeic acid, scutellarein, allixin, lauric acid and quercetin has two hydrogen bonds. L-cystein has 3 hydrogen bonds whereas 3-L-alanine, kaempferol and glutathione has 4 hydrogen bonds. Maximum hydrogen bonds are shown by fructan, myricetin and gamma-glutamyl-L-cysteine as 5 hydrogen bonds each [72, 73].

## 4.5 ADMET Properties of Ligands

Lipinski's five drug law used as a first step in assessing verbal bioavailability and artificial availability. A second study was performed by calculating the ADMET properties of ligands as a measure of pharmacokinetics using the online tool pkCSM. In pharmacology there two broad terms the one is pharmacodynamics and the other is pharmacokinetics [79]. In our thesis, 25 different ligands were taken and when filtered by different softwares, few are left. So, when lipaski rule of five was applied, Myricetin, Fructan, Linoleic Acid, Ethyl Linoleate, Glutathione and S-Allyl-Mercapto-Glutathione are knocked out as shown in the Table 4.4.

### 4.5.1 Pharmacodynamics

Pharmacodynamics is a branch of pharmacology in which we study the effect of drugs on the body [80].



## 4.5.2 Pharmacokinetics

It is a branch of pharmacology in which we study drug's effect. In pharmacokinetics we study the absorption of drugs, distribution of drugs, metabolism of the drug and excretion of the drugs [80].

TABLE 4.3: ADMET properties (lipaski's rule of five) [79].

Sr. No	Ligand	LogP	Molecular Weight (g/mol)	Hydrogen Bond Acceptor	Hydrogen Bond Donor
1	3-(Allylsulphinyl)-L-Alanine	-0.667	177.225	3	2
2	Allicin	1.7553	162.279	2	0
3	Diallyl Sulfide	2.0916	114.213	1	0
4	Diallyl Disulfide	2.7398	146.28	2	0
5	Diallyl Trisulfide	3.388	178.347	3	0
6	Glutathione	-2.2061	307.328	6	6
7	L-Cysteine	-0.6719	121.161	3	3
8	S-Allyl-Mercapto-Glutathione	-0.741	379.46	7	6
9	Thiocysteine	-0.0237	153.228	4	3
10	Gamma-Glutamyl-L-Cysteine	-0.0227	429.503	10	6
11	Gamma-Glutamyl-S-Allylcysteine	-0.3329	290.341	5	4
12	Kaempferol	2.2824	286.239	6	4
13	Quercetin	1.988	302.238	7	5
14	Myricetin	1.6936	318.237	8	6
15	Fructan	-7.5682	504.438	16	11
16	Lauric Acid	3.9919	200.322	1	1
17	Linoleic Acid	5.8845	280.452	1	1
18	Allixin	2.39512	226.272	4	1

---

19	Ajoene	3.0022	234.411	3	0
20	Ethyl Linoleate	6.363	308.506	2	0
21	Diazinon	3.58472	304.352	6	0
22	Levamisole	2.1461	204.298	3	0
23	Scutellarein	2.2824	286.239	6	4
24	S-allylcysteine methylester	1.9719	275.37	5	1
25	Caffeic acid	2.987	180.159	3	3

---

## 4.6 Absorption

In pharmacology (specifically pharmacokinetics), the transfer of a drug from the bloodstream into the tissues is called absorption and drug's composition and surrounding environment is used to detect the rate of absorption [83].

Absorption is one of ADME properties which predict absorption of orally administered drugs and includes Water solubility, CaCO<sub>2</sub> permeability, Intestinal absorption, Skin permeability, P-glycoprotein substrate, and P-glycoprotein I & II inhibitors. Water solubility (log S) of a compound predicts its solubility in water at 25°C. It is predicted as a molar concentration logarithm (log mol/L). Lipid soluble drugs are less soluble in water than water-soluble drugs [84]. The CaCO<sub>2</sub> permeability model detects the logarithm of the apparent permeability coefficient (log P<sub>app</sub>; log cm/s). A compound has a high CaCO<sub>2</sub> absorbency if it has a P<sub>app</sub> > 8 ÷ 10<sup>-6</sup> cm/s. Intestinal absorption predicts the percentage that will enter a person's small intestine. A compound with less than 30% absorption is considered to be less absorbent. The skin permeability model predicts the absorbency in log K<sub>p</sub> and this model has a special interest in the formation of transdermal drugs. The element with the log K<sub>p</sub> > -2.5 means it has low skin penetration [85].

The P-glycoprotein substrate behaves as natural barrier and removes unwanted toxins from the cells. This model predicts whether the given compound may be

P-glycoprotein (Pgp) substratum or not. This means if a compound is a Pgp substrate (categorically yes), it may be show low oral absorption. Pgp substrates can be easily pumped out of the cells to reduce their absorption [86].

Glycoprotein I/II inhibitor model predicts that the compound is likely to be a P-gb I/II inhibitor or not. Pgp inhibitors reduce the pumping activity of Pgp and may have high absorption as shown in the Table 3 (refer to Appendix C).

## 4.7 Distribution

It is a branch of pharmacokinetics in which we deals with the movement of the drugs within the body from one to another location and place. Distribution as one of ADME property includes four models namely as Volume of distribution in human (VD<sub>ss</sub> expressed as log L/kg), Fraction unbound in humans (Fu), Blood brain barrier (BBB) permeability expressed as log BB, and Central nervous system permeability (CNS permeability) expressed as log PS [87].

It is a branch of pharmacokinetics in which we deals with the movement of the drugs within the body. Model-1 explains the theoretical volume that the total amount of drug will need to be evenly distributed to provide the same concentration as in blood plasma. VD<sub>ss</sub> is considered low if it is less than 0.71 L /kg (log VD<sub>ss</sub> < 0.15) and higher if it is above 2.81L / kg (log VD<sub>ss</sub>> 0.45). If VD<sub>ss</sub> is high, it means that more of the drug is still distributed to the tissues than to plasma [88]. If a compound shows more Fu value, its mean it is more effective. BBB protects the brain from exogenous compounds so BBB permeability is an important parameter.

If predicted value of log BB >0.3 then its mean given substance can cross BBB and if value <-1 then no harm to brain. Log PS is the product of blood-brain permeability and surface area, and its value >-2 considered to penetrate the Central Nervous System (CNS), and <-3 considered as safe [89]. Table 4.4 shows distribution properties of selected ligands.

TABLE 4.4: Distribution properties of ligands [89].

Sr. No.	Ligand	VD <sub>ss</sub> (human)	Fraction Unbound (human)	BBB permeability (human)	CNS permeability
1	3-(Allylsulphinyl)	-0.553	0.462	-0.271	-3.472
2	Allicin	-0.045	0.577	0.506	-2.312
3	Diallyl Sulfide	0.202	0.552	0.69	-2.102
4	Diallyl Disulfide	0.211	0.518	0.78	-2.21
5	Diallyl Trisulfide	0.216	0.483	0.767	-2.309
6	Glutathione	-0.377	0.463	-1.085	-3.903
7	L-Cysteine	-0.486	0.49	-0.398	-3.476
8	S-Allyl-Mercapto	-1.517	0.588	-1.475	-4.217
9	Thiocysteine	-0.501	0.47	-0.376	-3.5
10	Gamma-Glutamyl	-0.203	0.495	-1.994	-4.159
11	Gamma-Glutamyl-S-Allylcysteine	-0.48	0.452	-1.124	-4.02
12	Kaempferol	1.274	0.178	-0.939	-2.228
13	Quercetin	1.559	0.206	-1.098	-3.065
14	Myricetin	1.317	0.238	-1.493	-3.709
15	Fructan	-0.276	0.499	-1.886	-4.815
16	Lauric Acid	-0.631	0.26	0.057	-2.034
17	Linoleic Acid	-0.587	0.054	-0.142	-1.6
18	Allixin	-0.008	0.479	0.193	-2.86
19	Ajoene	0.083	0.395	0.703	-2.178
20	Ethyl Linoleate	0.306	0.015	0.776	-1.562
21	Diazinon	-0.348	0.329	-0.438	-3.029
22	Levamisole	0.428	0.358	0.358	-2.011
23	Scutellarein	0.587	0.192	-1.398	-2.363
24	S-allylcysteine	-0.396	0.434	-0.119	-2.911
25	Caffeic acid	-1.098	0.529	-0.647	-2.608

## 4.8 Metabolism

CYP1A2, CYP2C19, CYP2C9, CYP2D6, and CYP3A4 models of the various isoforms of Cytochrome P450 which is an important cleansing enzyme found in the liver.

This enzyme reacts to xenobiotics to facilitate their release. Some drugs are triggered by this enzyme while most drugs are neutralized by it [87]. Table 4.5 shows metabolism models of our selected ligands.

TABLE 4.5: Parameters measuring metabolism of ligands [87].

Sr. No	Ligand	CYP-2D6 substrate	CYP-3A4 substrate	CYP-2D6 inhibitor	CYP-2C19 inhibitor	CYP-2C9 inhibitor	CYP-2D6 inhibitor	CYP-3A4 inhibitor
1	3-(Allylsulphanyl)-L-Alanine	No	No	No	No	No	No	No
2	Allicin	No	No	No	No	No	No	No
3	Diallyl Sulfide	No	No	No	No	No	No	No
4	Diallyl Disulfide	No	No	No	No	No	No	No
5	Diallyl Trisulfide	No	No	No	No	No	No	No
6	Glutathione	No	No	No	No	No	No	No
7	L-Cysteine	No	No	No	No	No	No	No
8	S-Allyl-Mercapto-Glutathione	No	No	No	No	No	No	No
9	Thiocy-steine	No	No	No	No	No	No	No



## 4.9 Excretion

The organs involved in drug excretion are the kidneys, which play important role in renal excretion and the biliary excretion. Some more organs may also be involved in the process of excretion, for example lungs are used for volatile or gaseous agents. Moreover Drugs can also be excreted through many means including sweat, saliva and tears. Models of Excretion property are Total Clearance (CL tot) expressed as log (CL tot) in ml/min/kg and second one is Renal OCT2 substrate which predicts results as Yes /No. OCT2 (organic cation transporter 2) is a renal uptake transporter which plays role in disposition and renal clearance of drugs [88, 89]. All ligands showed negative result for model Renal OCT2 substrate. Excretory properties are listed in Table 4.6

TABLE 4.6: Excretion properties of ligands [89].

Sr. No.	Ligand	Total Clearance	Renal OCT2 Substrate
1	3-(Allylsulphinyl)-L-Alanine	0.365	No
2	Allicin	0.714	No
3	Diallyl Sulfide	0.555	No
4	Diallyl Disulfide	0.547	No
5	Diallyl Trisulfide	0.446	No
6	Glutathione	0.308	No
7	L-Cysteine	0.53	No
8	S-Allyl-Mercapto-Glutathione	0.333	No
9	Thiocysteine	0.369	No
10	Gamma-Glutamyl-L-Cysteine	0.159	No
11	Gamma-Glutamyl-S-Allylcysteine	0.3	No

---

12	Kaempferol	0.477	No
13	Quercetin	0.407	No
14	Myricetin	0.422	No
15	Fructan	1.516	No
16	Lauric Acid	1.623	No
17	Linoleic Acid	1.936	No
18	Allixin	0.419	No
19	Ajoene	0.538	No
20	Ethyl Linoleate	2.08	No
21	Diazinon	0.391	No
22	Levamisole	0.475	No
23	Scutellarein	0.47	No
24	S-allylcysteine methylester	0.487	No
25	Caffeic Acid	0.508	No

---

## 4.10 Toxicity Prediction

The maximum tolerated dose (MRTD) provides a measure of toxic chemical limits on individuals. This will help in directing the first recommended dose of the treatment regimen in phase 1 clinical trials. MRTD is expressed in the form of logarithms ( $\log \text{ mg/kg/day}$ ). If in a given compound value of MRTD is less than or equal to  $0.477 \log (\text{mg/kg/day})$  it is considered to be lower and higher if it is higher than  $0.477 \log (\text{mg/kg/day})$ . The hERG I & II inhibitors model is said to cause inhibit the potassium channels induced by the h ERG which are the main causes of the development of chronic QT syndrome leading to fatal ventricular arrhythmia. The inhibition of h ERG channels has led to the withdrawal of many items from the pharmaceutical market. LD50 is the quantity of a compound that causes the deaths of 50% of experimental animals (mice) [90, 91]. The LD50 ( $\text{mol/kg}$ ) predicts toxicity of a probable compound where as LOAEL aims to identify the



lowest dosage of a compound with a significant adverse effect. Exposure to low to moderate chemical doses for a long time is very important in medicine and is expressed in a log (mg/kg-bw/day)[92]. *T. pyriformis* is a protozoan's bacteria, whose toxin is often used as a toxic endpoint (IGC50) and inhibits 50% growth. p IGC50 (negative concentration logarithm required to prevent 50% growth) in log ug / L predicted value  $> -0.5 \log \text{ ug/L}$  is considered toxic.

The lethal concentrations (LC50) represent the concentration of molecules needed to cause the death of 50% of Flathead Minnows (small bait shes). In Minnow toxicity LC50 values below 0.5 m M ( $\log \text{ LC } 50 < -0.3$ ) are regarded as high acute toxicity [93,94]. Toxicity predicted values of selected ligands were listed in Table 4.7.

TABLE 4.7: Predicts toxicity of ligands [93].

Ligand	Max. tolerated dose (human) mg/Kg	hE RG I inhibitor	hE RG II inhibitor	Oral rat acute toxicity	Oral rat chronic toxicity	He-pa-toxicity	Sk-in Sensi-tion	t.py-riformis toxicity	Minnow toxicity
3-(Allylsulphanyl)-L-Alanine	1.164	No	No	2.0 51	1.9	No	No	0.2 68	2.5 98
Allicin	0.737	No	No	2.3 66	1.4 06	No	Yes	0.9	1.2 35
Diallyl Sulfide	0.782	No	No	2.0 28	1.8 12	No	Yes	0.63	1.1 54
Diallyl Disulfide	0.674	No	No	2.3 75	1.8 47	No	Yes	1.3 71	0.79
Diallyl Trisulfide	0.582	No	No	2.7 11	1.8 57	No	Yes	2.0 08	0.5 16

Glutathione	1.104	No	No	2.4 68	2.9 19	No	No	0.2 85	4.5 69
L-Cysteine	1.133	No	No	1.9 82	2.6	No	No	0.1 49	2.9 92
S-Allyl-Mercapto-Glutathione	1.196	No	No	1.8 04	2.9 02	Yes	No	0.2 85	4.1 64
Thiocysteine	1.113	No	No	1.9 83	2.2 75	No	No	0.1 01	2.6 57
Gamma-Glutamyl-L-Cysteine	0.856	No	No	2.4 78	3.3 61	Yes	No	0.2 85	4.3 06
Gamma-Glutamyl-S-Allyl-cysteine	1.119	No	No	2.4 38	2.29	No	No	0.2 85	2.9 28
Kaempferol	0.531	No	No	2.4 49	2.5 05	No	No	0.3 12	2.8 85
Quercetin	0.499	No	No	2.4 71	2.6 12	No	No	0.2 88	3.7 21
Myricetin	0.51	No	No	2.4 97	2.7 18	No	No	0.2 86	5.0 23
Fructan	0.667	No	Yes	2.7 75	4.7 03	No	No	0.2 85	13.2 91
Lauric Acid	-0.34	No	No	1.5 11	2.89	No	Yes	0.9 54	-0.0 84
Linoleic Acid	-0.827	No	No	1.4 29	3.1 87	Yes	Yes	0.7 01	-1.31

Allixin	0.879	No	No	2.1 95	1.7 55	No	No	0.3 24	1.5 82
Ajoene	0.462	No	No	2.4 72	0.8 99	No	Yes	2.1 97	0.1 55
Ethyl Linol- eate	0.009	No	No	1.6 44	3.0 25	No	Yes	1.4 97	-1.7 65
Diazi- non	1.362	No	No	3.2 58	0.9 53	Yes	No	0.3 66	-0.1 48
Levam- isole	0.035	No	No	2.7 11	1.5 48	No	Yes	1.3 55	1.45
Scutel- larein	0.626	No	No	2.4 52	3.1 35	No	No	0.3 01	1.99
S-allyl- cysteine methyl- ester	0.703	No	No	2.6	0.9 08	No	No	0.9 13	1.1 12
Caffeic Acid	1.145	No	No	2.3 83	2.0 92	No	No	0.2 93	2.2 46

## 4.11 Lead Compounds Identification

Physicochemical and Pharmacokinetics properties determine the final destiny of compounds as drug or non-drug compounds. Physicochemical properties or Lipinski's rule of five works as primary filter and Pharmacokinetics studies as secondary filter in screening of potential compounds [93]. Myricetin, Fructan, Linoleic Acid, Ethyl Linoleate, Glutathione and S - Allyl- Mercapto- Glutathione are knocked out from lipanski's rule of five. 3- (Allylsulphiny) - L - Alanine, Scutellarein, Diazinon, Glutathione, L-Cysteine, S-Allyl-Mercapto - Glutathione, Thiocysteine, Kaempferol, Quercetin, Myricetin Fructan, Lauric Acid, Linoleic Acid, Allixin,

Gamma-Glutamyl-L-Cysteine, Gamma-Glutamyl-S-Allylcysteine, S-allylcysteine methylester, Caffeic Acid has the logBB value  $>0.3$ . 3-(Allylsulphinyl)-L-Alanine, Scutellarein, Diazinon, Glutathione, L-Cysteine, Gamma-Glutamyl-S-Allylcysteine, S-allylcysteine methylester, Caffeic Acid, S-Allyl- Mercapto - Glutathione, Thio-cysteine, Gamma-Glutamyl-L-Cysteine, Kaempferol, Quercetin, Myricetin Fructan, Lauric Acid, Linoleic Acid, Allixin and Ethyl Linoleate has the logBB value  $>0.3$  and logPS value  $>-2$ .

Linoleic Acid, Ethyl Linoleate has logPS value  $>-2$  So, the lig can be identified as lead compounds. Best five compounds (Hit compounds on the basis of primary and secondary filters, toxicity predicted values and binding score) are and Allicin, Diallyl Sulfide, Diallyl Disulfide, Diallyl Trisulfide, Ajoene and Levamisole. (Binding scores with all three receptors shown in Table 4.5). Lead Compound of this research work is Levamisole as it is also indicated by molecular docking [95].

## 4.12 Drug Identification Against Covid-19

With the emergence of the disease, many FDA-approved drugs were utilized for drug repurposing finding the best treatment against the virus. One of the drugs that have been in use in different countries like the UK, Brazil, India, Pakistan, and many more is Remdesivir. Though the use of this medicine has increased during this whole pandemic this drug is still in clinical trials [50, 51].

### 4.12.1 Remdesivir

Remdesivir was the first drug approved by the FDA to treat the SARS-CoV-2 virus. The broad-spectrum antiviral is a nucleotide analog prodrug [52]. Remdesivir is an adenosine triphosphate analogue first successful treatment for Ebola virus. Because of its mechanism of action and invitro activity against the Arenaviridae, Flaviviridae, Filoviridae, Paramyxoviridae, Pneumoviridae, and Coronaviridae viral families, it is suggested to the patients. As in 2017, it is suggested

against corona viridae family so it is then suggested against corona virus. This medicine is non-obligate chain terminator of RdRp from SARS-CoV-2 and the related SARS-CoV and MERS-CoV, and has been investigated and suggested in many different clinical trials against Covid-19 [53].

## 4.13 Drug ADMET Properties

The drug ADMET properties are studied by using the same software as above which is pkCSM.

### 4.13.1 Toxicity prediction of Reference Drug

Table 4.8 shows the Toxicity Properties of Remdesivir. Toxicity parameters value of Remdesivir shows that this drug can be toxic towards liver but other parameters are in the range of positive values.

Which indicates that Remdesivir can cause any sensitivity to skin and it also is not a inhibitor of hERG I but hERG II inhibitor. The dose value of 0.291 is also tolerable. With that a no to AMES toxicity indicates that it is not carcinogenic.

TABLE 4.8: Toxicity properties of Remdesivir

Ligand	Max. Tolerated Dose (Human)	Hergr I Inhibitor	Hergr II Inhibitor	Oral Rat Acute Toxicity	Oral Rat Chronic Toxicity	Hergr toxicity	Skin Sensitization	T.Pyrimis Toxicity	Minnow Toxicity (Log Mm)
Remdesivir	1.9 72	No	Yes	2.0 43	1.6 39	Yes	No	0.2 85	0.2 91

### 4.13.2 Absorption Properties

Table 4.9 shows the absorption properties of Remdesivir. The values show that Remdesivir shows a very low  $\text{CaCO}_2$  solubility and water solubility. Though the intestinal absorption is high but it still is in the safe range. Remdesivir also has a lower value of skin permeability. Remdesivir is also a P-glycoprotein substrate and an inhibitor to P-glycoprotein I but not a P-glycoprotein II inhibitor.

TABLE 4.9: Absorption properties of Remdesivir

Ligands Name	Water Solub- ility	$\text{CaCO}_2$ Perme- ability	Intes- tinal Absor- ption (human)	Skin Perme- ability	P-glu- co pr- otein Sub- strate	P-glu- co pr- otein I Inhi- bitor	P-glu- co pr- otein II Inhi- bitor
Remd- esivir	-3.07	0.635	71.109	-2.735	Yes	Yes	No

### 4.13.3 Distribution Properties

Table 4.10 shows the distribution properties of Remdesivir. The distribution parameters value shows that the value of  $\text{VD}_{ss}$  is low which means the drug would not be distributed properly. Remdesivir can penetrate in CNS and also can pass the blood brain barrier.

TABLE 4.10: Distribution properties of Remdesivir

Sr. No	Name	$\text{VD}_{ss}$ (human)	Fractionun Bound (human)	BBB Permeability (human)	CNS permeability
1	Remdesivir	0.307	0.005	-2.056	-4.675

#### 4.13.4 Metabolic Properties

Table 4.11 shows the metabolic properties of Remdesivir. It indicates that Remdesivir is not a CYP2D6 substrate rather than it is a CYP3A4 substrate. With that table 4.14 shows that Remdesivir is not a CYP1A2, CYP2C19, CYP2C9, CYP2D6 and CYP3A4 inhibitor.

TABLE 4.11: Metabolic properties of Remdesivir

Sr. No	Ligand Name	CYP-2D6 subs- trate	CYP-3A4 subs- trate	CYP-2D6 inhi- bitor	CYP-2C19 inhi- bitor	CYP-2C9 inhi- bitor	CYP-2D6 inhi- bitor	CYP-3A4 inhi- bitor
1	Remdesivir	No	Yes	No	No	No	No	No

#### 4.13.5 Excretion Properties

Table 4.12 shows the excretion properties of Remdesivir. The above table gives the values of Excretory properties of Remdesivir. It shows that Remdesivir is not a renal OCT2 Substrate which means it will not help in clearing of the drug. With that the value of total clearance as 0.198 is also given with respect to its liver.

TABLE 4.12: Excretion properties of Remdesivir

Sr. No	Ligand Name	Total Clearance	Renal OCT2 Substrate
1	Remdesivir	0.198	No

### 4.14 Remdesivir Mechanism of Action

Using polymerase enzymes from the coronavirus that causes MERS, scientists in Götte's lab found that the enzymes can incorporate remdesivir, which resembles an

RNA building block, into new RNA strands. Shortly after adding remdesivir, the enzyme stops being able to add more RNA subunits. This halts genome replication [96]. The protein encoded by this gene belongs to the angiotensin-converting enzyme family of dipeptidyl carboxydipeptidases and has considerable homology to human angiotensin 1 converting enzyme. This secreted protein catalyzes the cleavage of angiotensin I into angiotensin 1-9, and angiotensin II into the vasodilator angiotensin 1-7. The organ- and cell-specific expression of this gene suggests that it may play a role in the regulation of cardiovascular and renal function, as well as fertility [97, 98]. In addition, the encoded protein is a functional receptor for the spike glycoprotein of the human coronavirus HCoV-NL63 and the human severe acute respiratory syndrome coronaviruses, SARS-CoV and SARS-CoV-2 [99]. Mechanism of action of drug is shown in Figure 4.33.

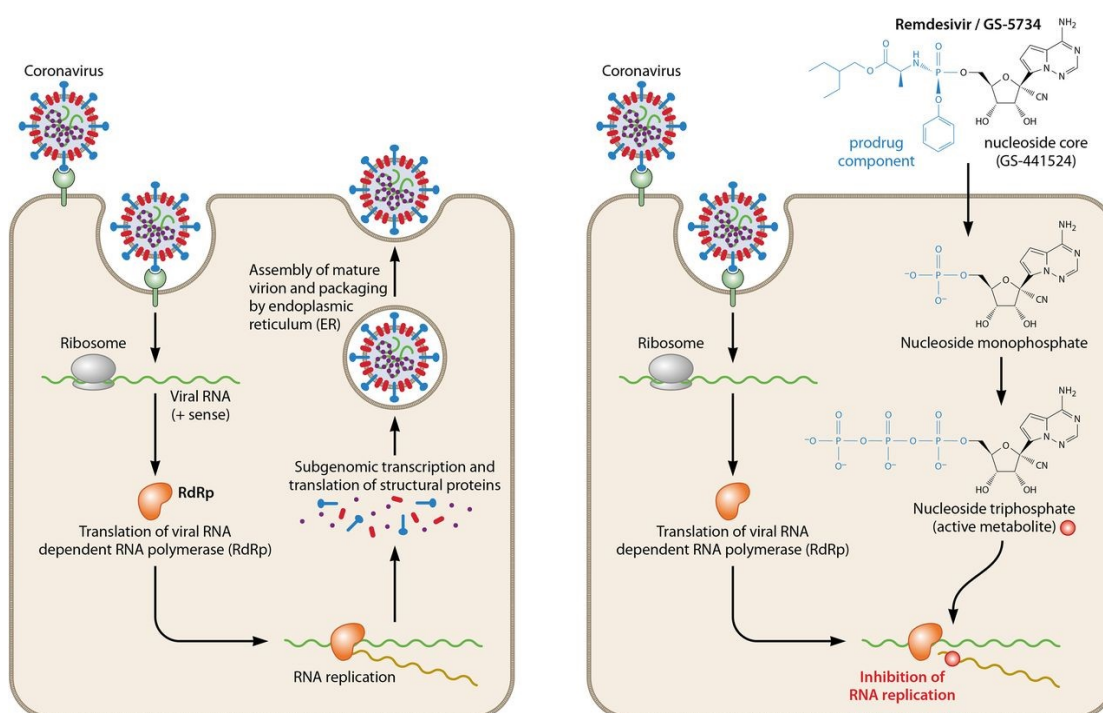


FIGURE 4.33: Mechanism of Action of Remdesivir Drug.

## 4.15 Remdesivir Molecular Docking

Table 4.13 shows the docking result of Remdesivir. The table indicates that azithromycin has a binding score of -8.1. The docking results of Remdesivir shows



that it has quite a good binding score. And has four hydrogen bond donors, and thirteen hydrogen bond acceptors that breaks two of Lipinski rule as the molecular weight is above 500 g/mol.

TABLE 4.13: Docking result of Remdesivir

Sr. No	Name	Bind- ing Score	Cavity Size	Grid Map	HBA	HBD	logP	Mol. Weight g/mol
1	Remd- esivir	-8.1	1385	22	13	4	2.31 218	602. 585

## 4.16 Remdesivir Comparison with Lead Compound

The standard drug Remdesivir is compared with the lead compound Levamisole and their physicochemical and pharmacokinetic properties. The Table 4.17 shows that Remdesivir breaks two of Lipinski's rules that are of molecular weight and H-bond acceptor as the molecular weight of Remdesivir is 602.585 which is more than 500 according to Lipinski and that for Hbond acceptor Remdesivir accepts 13 hydrogens but according to Lipinski it should not be more than 10, whereas Levamisole follows all rules of LogP, Molecular weight, H-bond acceptor and H-bond donor according to Lipinski.

TABLE 4.14: Remdesivir comparison with lead compound

Sr. No	Ligand	LogP	Molecular Weight (g/mol)	Hydrogen Bond Acceptor	Hydrogen Bond Donar
1	Remdesivir	2.31218	602.585	13	4
2	Levamisole	2.1461	204.29	3	0

## 4.17 ADMET Properties Comparison

The ADMET properties comparison is done to check the absorption, distribution, metabolic excretion, and toxicity properties of the drug and the lead compound for finding a better drug candidate.

### 4.17.1 Toxicity Comparison

The toxicity of both the standard drug and lead compound is based upon 9 models. Model 1 of AMES toxicity shows that both the standard and lead compounds are not mutagenic. Model 2 of Maximum tolerated dose gives that if the value is equal or less to 0.477 log mg/kg/day then it is considered low and greater values are considered high.

The Table 4.15 below shows that Levamisole has a low value of tolerated dose. 3rd model is of hERG I and II inhibitors, only levamisole is inhibitor of both while remdesivir inhibit only II inhibitor.

4th model of oral rat acute toxicity is used to assess the relative toxicity. Model 5 of oral rat chronic toxicity gives the values of the lowest dose that could result in an adverse effect. Model 6 of hepatotoxicity shows either the drug can cause damage to the liver.

The Table shows that Remdesivir is hepatotoxic. For the dermal products model, 7 is used for checking the sensitivity towards the skin. Both the standard and lead compounds are not sensitive to skin. Model 8 uses *T. pyriformis* and model 9 uses minnows to check the toxicity.

For *T. pyriformis* value  $> -0.5$  is considered toxic according to which Remdesivir is somewhat toxic and for minnow toxicity values below 0.5mM are considered toxic and both compounds pass this toxicity test. Table 4.15 shows the comparative values of toxicity of Remdesivir and Levamisole.

TABLE 4.15: Comparative values of toxicity of Remdesivir and Levamisole

Lig- and	Max.	Oral			Oral	He-		T.Py-	Min- now Tox- icity (Log Mm)
	Toler- ated Dose (Hu- man) (mg/ Kg)	He- rg I Inh- ibi- tor	Her- g II Inh- ibi- tor	Rat Acu- te To- xicity (mol/ Kg)	Rat Chr- onic Tox- icity (mol/ Kg)	pa- tox- ici- ty	Skin Sen- sitis- ation	rifor- mis Toxi- city (Log Ug/ L)	
Remd- esivir	0.196	No	Yes	2.043	1.639	Yes	No	0.285	0.291
Levam- isole	0.035	No	No	2.711	1.548	No	Yes	1.355	1.45

#### 4.17.2 Absorption Properties Comparison

The parameter of absorption is based upon 6 models. The water solubility model gives the value of compound's solubility in the water at 25°C. Model of CaCO<sub>2</sub> solubility is used to detect the absorption of drug. Values greater than 0.90 are considered to have high intestinal absorption, which means Levamisole is absorbed more than Remdesivir. Value of Intestinal absorption model less than 30% is means drug is not well absorbed. The given values of both the standard and lead compound show that Levamisole has high intestinal absorption.

For the transdermal drugs the skin permeability model, value less than  $\log K_p > -2.5$  is considered low, according to this both the compounds pass the skin permeability test. The P-glycoprotein substrate model is very important as P-glycoprotein is an ABC transporter. Both Levamisole and Remdesivir act as the substrates. The last model of P-glycoprotein inhibitors shows that whether the compound is an inhibitor or not. The Table 4.16 shows that Levamisole is an

inhibitor of P-glycoprotein II whereas Remdesivir is the inhibitor of P-glycoprotein I.

TABLE 4.16: Comparative values of absorption of Remdesivir and Levamisole

Ligands Name	Water Solubility	CaCO <sub>2</sub> Permeability	Intestinal absorption (human)	Skin Permeability	P-glycoprotein substrate	P-glycoprotein I Inhibitor	P-glycoprotein II Inhibitor
Remdesivir	-3.07	0.635	71.109	-2.735	Yes	Yes	No
Levamisole	-3.173	1.491	93.678	-2.075	No	No	No

### 4.17.3 Metabolic Properties Comparison

Cytochrome P450 is found in the liver mainly and is held responsible for oxidizing the xenobiotic so that they can be excreted easily out from the body hence making cytochrome P450 a detoxification enzyme. Some drugs are activated by it or some are deactivated. The Table 4.14 shows that Remdesivir is a CYP3A4 substrate and Levamisole is a CYP3A4 substrate and CYP2D6 inhibitor.

TABLE 4.17: Comparative values of metabolic properties of Remdesivir and Levamisole

Ligand Name	CYP-2D6 substrate	CYP-3A4 substrate	CYP-2D6 inhibitor	CYP-2C19 inhibitor	CYP-2C9 inhibitor	CYP-2D6 inhibitor	CYP-3A4 inhibitor
Remdesivir	No	Yes	No	No	No	No	No
Levamisole	No	No	Yes	No	No	Yes	No

#### 4.17.4 Distribution Properties Comparison

Table 4.18 shows the comparative distribution properties of Remdesivir and Levamisole. The distribution parameter is based upon 4 models. The volume of distribution (VDss) is uniform distribution of drug in the blood plasma and if this value is above 2.81 L/kg then the drug is distributed more in the tissues rather than in the blood plasma. Both Remdesivir and Levamisole have a reasonable VDss value. 2nd model is based upon the fraction unbound of the drugs in the plasma as bounded drugs affect the efficiency of the drugs. The given value is the amount of the drug which remains unbound. For BBB permeability if the value is greater than 0.3 logBB then that drug can easily cross the blood-brain barriers and if the value is less than -1 logBB then the drug does not reach brain in proper manner. By these values, it is clear that Remdesivir has a low value hence it would be poorly distributed to the brain. Similarly, the model for CNS is based on the values that if the logPS > -2 then that drug can easily penetrate to the CNS while those having value of logPS < -3 are unable to reach the CNS. Remdesivir has a low value hence it will not cross and reach to the CNS.

TABLE 4.18: Comparative values of distribution of Remdesivir and Levamisole

Sr. No	Name	VDss (human)	Fraction unbound (human)	BBB permeability (human)	CNS permeability
1	Remdesivir	0.307	0.005	-2.056	-4.675
2	Levamisole	0.428	0.358	0.358	-2.011

#### 4.17.5 Excretion Properties Comparison

Levamisole has more total clearance than Remdesivir. The 2nd model is of the Renal OCT2 (organic cation transporter 2) and this transporter helps in the renal clearance. Being an OCT2 substrate can show an adverse effect in correlation with

inhibitors. So both Remdesivir and Levamisole are not Renal OCT2 substrates. Table 4.19 shows the values of excretory properties of Remdesivir and Levamisole.

TABLE 4.19: Values of excretory properties of Remdesivir and Levamisole.

Sr. No.	Ligand Name	Total clearance	Renal OCT2 substrate
1	Remdesivir	0.198	No
2	Levamisole	0.475	No

## 4.18 Physiochemical Properties Comparison

For determining the fundamental properties of the compounds physiochemical properties are studied. Through this screening, it shows that Remdesivir has 27 carbon atoms, 35 hydrogen atoms, 6 nitrogen atoms, and 8 oxygen atoms and phosphorous atom whereas Levamisole has 11 carbon atoms, 12 hydrogen atoms, and 2 nitrogen atoms and Sulphur. Remdesivir can donate 4 hydrogen atoms whereas Levamisole can't donate hydrogen.

Remdesivir can accept 13 Hydrogen atoms which do not fall under the Lipinski rule. Although the Log P value of Remdesivir is more than Levamisole the molecular weight of Remdesivir is far greater than Levamisole and also it does not fall under the Lipinski rule. Table 4.20 shows the comparison of physiochemical properties of Remdesivir and Levamisole.

TABLE 4.20: Comparison of physiochemical properties of Remdesivir and Levamisole

Sr. No.	Ligand	LogP	Molecular Weight (g/mol)	Molecular Formula	H-Bond Acceptor	H-Bond Donar
1	Remdesivir	2.31218	602.585	C <sub>27</sub> H <sub>35</sub> N <sub>6</sub> O <sub>8</sub> P	13	4
2	Levamisole	2.1461	204.29	C <sub>11</sub> H <sub>12</sub> N <sub>2</sub> S	3	0

## 4.19 Docking Score Comparison

Both the standard and the lead compound were docked and the docking result gives us the best binding score. Table 4.24 shows that the lead compound Levamisole which is has a much higher vina score than that of the standard drug which is Remdesivir. The binding score of Remdesivir is -8.1 and that for Levamisole is -5.7 which is higher. This result shows that Levamisole can block the Mpro or bind with it more efficiently than that of Remdesivir.

TABLE 4.21: Docking Score Comparison

S.No	Name	Binding Score
1	Remdesivir	-8.1
2	Levamisole	-5.7

## Chapter 5

# Conclusion and Future Prospects

The motive of the present research was to discover potential antiviral components from *Allium sativum*. Twenty five phyto compounds (which represent almost all classes of natural antiviral compounds) were selected from literature and databases. Molecular docking was performed by CB-dock online tool and five best scoring phytocompounds namely were identified as hit compounds. Physicochemical and Pharmacokinetics properties determined the final destiny of compounds as drug or non-drug compounds.

Levamisole was predicted as lead compound by virtual screening results. Lead compound levamisole as per this research results can be explored as an important candidate to cure viral infections especially covid. For the cure of viral, bacterial and parasitic infections, Levamisole is mostly used. All hit and lead compounds can also be tested as natural antioxidants for their efficiency and toxicity than synthetic ones. These potential antiviral compounds of *Allium sativum* can also be tested for the pharmaceutical and medical industries. Today world turns again towards natural sources in order to determine lead compounds for more effective, non-resistant, with lesser or no side effects drugs. It's proper time to secure our future by scientific novel antiviral compounds which would be stronger drug targets of the near future for these diseases. This work would be beneficial for everybody as it will be helpful in preventing viral diseases which are spreaded world widely.



# Bibliography

1. Aljabre, S.H., O.M. Alakloby, and M.A. Randhawa, Dermatological effects of Allium sativum. *Journal of dermatology & dermatologic surgery*, 2015. 19(2): p. 92-98.
2. Durrani, F., et al., Effect of Different Levels of Feed Added Garlic(.Allium sativum). *Pakistan Journal of Biological Sciences*, 2007. 10(22): p. 4164-4167.
3. Mahboubi, M., Natural therapeutic approach of Garlic(Allium sativum) fixed oil in management of Sinusitis. *Integrative medicine research*, 2018. 7(1): p. 27-32.
4. Umar, S., et al., Protective and antiviral activities of Garlic(Allium sativum) against avian influenza (H9N2) in turkeys. *J. Saudi Soc. agric. Sci*, 2016.9(2): p. 90-92.
5. Barakat, E.M.F., L.M. El Wakeel, and R.S. Hagag, Effects of Garlic(Allium sativum) on outcome of hepatitis C in Egypt. *World journal of gastroenterology: WJG*, 2013. 19(16): p. 2529.
6. Sahak, M.K.A., et al., The role of Garlic(Allium sativum) and its active constituents in learning and memory. *Evidence-Based Complementary and Alternative Medicine*, 2016. 11(1): p. 82-88.
7. Eid, A.M., et al., A Review on the Cosmeceutical and External Applications of Allium sativum. *Journal of tropical medicine*, 2017. 15(2): p. 67-69.

8. Forouzanfar, F., B.S.F. Bazzaz, and H. Hosseinzadeh, Garlic(*Allium sativum*): a review on antimicrobial effects. *Iranian journal of basic medical sciences*, 2014. 17(12): p. 929-933.
9. Ahmad, A., et al., A review on therapeutic potential of *Allium sativum*: A miracle herb. *Asian Pacific journal of tropical biomedicine*, 2013. 3(5): p. 337-352.
10. Marchese, A., et al., Update on monoterpenes as antimicrobial agents: A particular focus on p-cymene. *Materials*, 2017. 10(8): p. 947-955.
11. Zaher, K.S., W. Ahmed, and S.N. Zerizer, Observations on the biological effects of Garlic(*Allium sativum*) and green tea (*Camellia sinensis*). *Global Veterinaria*, 2008. 2(4): p. 198-204.
12. Shamim Molla, M., et al., A Review On Antiviral Effects Of Garlic . 2019.7 (5): p.223-227
13. Dinakaran, S., S. Sridhar, and P. Eganathan, Chemical composition and antioxidant activities of Garlic(*Allium sativum*). *International Journal of Pharmaceutical Sciences and Research*, 2016. 7(11): p. 4473-4476.
14. Sallehuddin, N., et al., *Nigella sativa* and Its Active Compound, Thymoquinone, Accelerate Wound Healing in an In Vivo Animal Model: A Comprehensive Review. *International Journal of Environmental Research and Public Health*, 2020. 17(11): p. 4160-4167.
15. Khader, M. and P.M. Eckl, Thymoquinone: an emerging natural drug with a wide range of medical applications. *Iranian journal of basic medical sciences*, 2014. 17(12): p. 950-956.
16. Al-Eidi, S., et al., Knowledge, attitude and practice of patients with type 2 diabetes mellitus towards complementary and alternative medicine. *Journal of integrative medicine*, 2016. 14(3): p. 187-196.
17. Hao, D.-C., *Ranunculales medicinal plants: biodiversity, chemodiversity and pharmacotherapy*. 2018: Academic Press.

18. Rasool Hassan, B., Medicinal plants (importance and uses). *Pharmaceut Anal Acta*, 2012. 3(10): p. 2153-2435.
19. Phillipson, J.D., *Phytochemistry and medicinal plants*. *Phytochemistry*, 2001. 56(3): p. 237-243.
20. Farnsworth, N.R. and D.D. Soejarto, *Global importance of medicinal plants. The conservation of medicinal plants*, 1991. 26: p. 25-51.
21. Qiu, J., *Traditional medicine: a culture in the balance*. 2007, Nature Publishing Group.
22. Saxena, M., et al., *Phytochemistry of medicinal plants. Journal of pharmacognosy and phytochemistry*, 2013. 1(6).
23. Kurmukov, A.G., *Phytochemistry of medicinal plants, in Medicinal Plants of Central Asia: Uzbekistan and Kyrgyzstan*. 2013, Springer. p. 13-14.
24. Rafieian-Kopaei, M., *Medicinal plants and the human needs. Journal of HerbMed Pharmacology*, 2012. 26(9): p. 25-35.
25. Verma, S. and S. Singh, *Current and future status of herbal medicines. Veterinary world*, 2008. 1(11): p.347-351.
26. Farnsworth, N.R. and D.D. Soejarto, *Global importance of medicinal plants. The conservation of medicinal plants*, 1991. 26: p. 25-51.
27. Qiu, J., *Traditional medicine: a culture in the balance*. 2007, Nature Publishing Group, 2007. 11(11): p.34-38.
28. Saxena, M., et al., *Phytochemistry of medicinal plants. Journal of pharmacognosy and phytochemistry*, 2013. 1(6):p.97-99.
29. Kurmukov, A.G., *Phytochemistry of medicinal plants, in Medicinal Plants of Central Asia: Uzbekistan and Kyrgyzstan*. 2013, Springer. p. 13-14.
30. Rafieian-Kopaei, M., *Medicinal plants and the human needs. Journal of HerbMed Pharmacology*, 2012.1(14):p.356-376.

31. Verma, S. and S. Singh, Current and future status of herbal medicines. *Veterinary world*, 2008. 1(11): p. 347-351.
32. Kavishankar, G., et al., Diabetes and medicinal plants-A review. *Int J Pharm Biomed Sci*, 2011. 2(3): p. 65-80.
33. Marchese, A., et al., Update on monoterpenes as antimicrobial agents: A particular focus on p-cymene. *Materials*, 2017. 10(8): p. 947-950.
34. Kulyar, M.F.-e.-A., et al., Potential influence of Garlic(*Allium sativum*) in reinforcing immune system: A hope to decelerate the COVID-19 pandemic. *Phytomedicine*, 2020.1(21): p. 153277-153281.
35. Zaher, K.S., W. Ahmed, and S.N. Zerizer, Observations on the biological effects of black cumin seed (*Nigella sativa*), Garlic(*Allium sativum*) and green tea (*Camellia sinensis*). *Global Veterinaria*, 2008. 2(4): p. 198-204.
36. Shamim Molla, M., et al., A REVIEW ON ANTIVIRAL EFFECTS OF Garlic(*Allium sativum*).2019.2(2):p.76-77.
37. Randhawa, M.A. and M.S. Al-Ghamdi, A review of the pharmaco-therapeutic effects of Garlic(*Allium sativum*).*Pak J Med Res*, 2002. 41(2): p. 77-83.
38. Sallehuddin, N., et al., *Nigella sativa* and Its Active Compound, Thymoquinone, Accelerate Wound Healing in an In Vivo Animal Model: A Comprehensive Review. *International Journal of Environmental Research and Public Health*, 2020. 17(11): p. 4160-4167.
39. Kamal, A., J.M. Arif, and I.Z. Ahmad, Potential of Garlic(*Allium sativum*) during different phases of germination on inhibition of bacterial growth. *J. Biotechnol. Pharm. Res*, 2010. 1(1): p. 9-13.
40. Khader, M. and P.M. Eckl, Thymoquinone: an emerging natural drug with a wide range of medical applications. *Iranian journal of basic medical sciences*, 2014. 17(12): p. 950-956.

41. Salman, M.T., R.A. Khan, and I. Shukla, Antimicrobial activity of Garlic(*Allium sativum*) oil against multi-drug resistant bacteria from clinical isolates. 2008.3(12):p.67-69
42. Al-Seeni, M.N., et al., The hepatoprotective activity of olive oil and Garlic(*Allium sativum*) oil against CCl<sub>4</sub> induced hepatotoxicity in male rats. BMC complementary and alternative medicine, 2016. 16(1): p. 438-440.
43. Sharma, N., et al., Medicinal and phamacological potential of Garlic(*Allium sativum*): a review. Ethnobotanical Leaflets, 2009. 2009(7): p. 11-16.
44. Dwivedi, S., et al., Satus and conservation strategies of endangered and vulnerable medicinal plants. *Planta Indica*, 2007. 3(2): p. 13-15.
45. Yessuf, A.M., Phytochemical extraction and screening of bio active compounds from Garlic(*Allium sativum*) extract. *American Journal of Life Sciences*, 2015. 3(5): p. 358-364.
46. Abdulelah, H. and B. Zainal-Abidin, In vivo anti-malarial tests of Garlic(*Allium sativum*) different extracts. *Am J Pharmacol Toxicol*, 2007. 2(2): p. 46-50.
47. Dinagaran, S., S. Sridhar, and P. Eganathan, Chemical composition and antioxidant activities of Garlic(*Allium sativum*) *International Journal of Pharmaceutical Sciences and Research*, 2016. 7(11): p. 4473-4477.
48. Cheikh-Rouhou, S., et al., *Nigella sativa* L.: Chemical composition and physicochemical characteristics of lipid fraction. *Food chemistry*, 2007. 101(2): p. 673-681.
49. Nergiz, C. and S. Ötles, Chemical composition of Garlic(*Allium sativum*). *Food chemistry*, 1993. 48(3): p. 259-261.
50. Schmutzhard, E., Viral infections of the CNS with special emphasis on herpes simplex infections. *Journal of neurology*, 2001. 248(6): p. 469-477.

51. Tregoning, J.S. and J. Schwarze, Respiratory viral infections in infants: causes, clinical symptoms, virology, and immunology. *Clinical microbiology reviews*, 2010. 23(1): p. 74-98.
52. Virgin, H.W., E.J. Wherry, and R. Ahmed, Redefining chronic viral infection. *Cell*, 2009. 138(1): p. 30-50.
53. Jacobs, S.R. and B. Damania, NLRs, inflammasomes, and viral infection. *Journal of leukocyte biology*, 2012. 92(3): p. 469-477.
54. Kawai, T. and S. Akira, Innate immune recognition of viral infection. *Nature immunology*, 2006. 7(2): p. 131-137.
55. Khan, A.U., et al., In-ovo antiviral effect of Garlic(*Allium sativum*) extract against Newcastle Disease Virus in experimentally infected chicken embryonated eggs. *Pakistan Veterinary Journal*,(2018),2018. 38: p. 434-437.
56. Mahmoud, M., H. El-Abhar, and S. Saleh, The effect of Garlic(*Allium sativum*) oil against the liver damage induced by *Schistosoma mansoni* infection in mice. *Journal of ethnopharmacology*, 2002. 79(1): p. 1-11.
57. Okeola, V.O., et al., Antimalarial and antioxidant activities of methanolic extract of *Nigella sativa* seeds (black cumin) in mice infected with *Plasmodium yoelli nigeriensis*. *Parasitology research*, 2011. 108(6): p. 1507-1512.
58. Nemmar, A., et al., Contrasting actions of diesel exhaust particles on the pulmonary and cardiovascular systems and the effects of thymoquinone. *British journal of pharmacology*, 2011. 164(7): p. 1871-1882.
59. Dias, R., J. de Azevedo, and F. Walter, Molecular docking algorithms. *Current drug targets*, 2008. 9(12): p. 1040-1047.
60. Yuriev, E. and P.A. Ramsland, Latest developments in molecular docking: 2010–2011 in review. *Journal of Molecular Recognition*, 2013. 26(5): p. 215-239.

61. Rani, G.J., M. Vinoth, and P. Anitha, Molecular docking studies on oxidosqualene cyclase with 4-piperidinopyridine and 4-piperidinopyrimidine as its inhibitors. *Journal of Bioinformatics and Sequence Analysis*, 2011. 3(3): p. 31-36.
62. Shoichet, B.K., et al., Lead discovery using molecular docking. *Current opinion in chemical biology*, 2002. 6(4): p. 439-446.
63. ul Qamar, M.T., et al., Computational screening of medicinal plant phytochemicals to discover potent pan-serotype inhibitors against dengue virus. *Scientific reports*, 2019. 9(1): p. 1- 16.
64. Thomsen, R. and M.H. Christensen, MolDock: a new technique for high-accuracy molecular docking. *Journal of medicinal chemistry*, 2006. 49(11): p. 3315-3321.
65. Pagadala, N.S., K. Syed, and J. Tuszynski, Software for molecular docking: a review. *Biophysical reviews*, 2017. 9(2): p. 91-102.
66. Bouchentouf, S. and N. Missoum, Identification of Compounds from *Nigella Sativa* as New Potential Inhibitors of 2019 Novel Coronasvirus (Covid-19): Molecular Docking Study. 2020. 4(2): p. 129-133.
67. De Serres, G., et al., Importance of viral and bacterial infections in chronic obstructive pulmonary disease exacerbations. *Journal of Clinical Virology*, 2009. 46(2): p. 129-133.
68. Cheng, J., M.J. Sweredoski, and P. Baldi, Accurate prediction of protein disordered regions by mining protein structure data. *Data mining and knowledge discovery*, 2005. 11(3): p. 213-222.
69. Roy, A., A. Kucukural, and Y. Zhang, I-TASSER: a unified platform for automated protein structure and function prediction. *Nature protocols*, 2010. 5(4): p. 725-738.

70. Pasi, M., et al., xPyder: a PyMOL plugin to analyze coupled residues and their networks in protein structures. *Journal of chemical information and modeling*, 2012. 52(7): p. 1865-1874.
71. Yuan, S., H.S. Chan, and Z. Hu, Using PyMOL as a platform for computational drug design. *Wiley Interdisciplinary Reviews: Computational Molecular Science*, 2017. 7(2): p. e1298.
72. Butkiewicz, M., et al., Benchmarking ligand-based virtual High-Throughput Screening with the PubChem database. *Molecules*, 2013. 18(1): p. 735-756.
73. Kim, S., et al., PubChem substance and compound databases. *Nucleic acids research*, 2016. 44(D1): p. D1202-D1213.
74. Kim, S., et al., PubChem 2019 update: improved access to chemical data. *Nucleic acid research*, 2019. 47(D1): p. D1102-D1109.
75. Ihlenfeldt, W.D., E.E. Bolton, and S.H. Bryant, The PubChem chemical structure sketcher. *Journal of cheminformatics*, 2009. 1(1): p. 1-9.
76. Brooijmans, N. and I.D. Kuntz, Molecular recognition and docking algorithms. *Annual review of biophysics and biomolecular structure*, 2003. 32(1): p. 335-373.
77. McConkey, B.J., V. Sobolev, and M. Edelman, The performance of current methods in ligand-protein docking. *Current Science*, 2002: p. 845-856.
78. Gschwend, D.A., A.C. Good, and I.D. Kuntz, Molecular docking towards drug discovery. *Journal of Molecular Recognition: An Interdisciplinary Journal*, 1996. 9(2): p. 175-186.
79. Wallace, A.C., R.A. Laskowski, and J.M. Thornton, LIGPLOT: a program to generate schematic diagrams of protein-ligand interactions. *Protein engineering, design and selection*, 1995. 8(2): p. 127-134



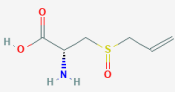
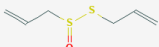



80. Morya, V.K., et al., In silico characterization of alkaline proteases from different species of *Aspergillus*. *Applied biochemistry and biotechnology*, 2012. 166(1): p. 243-257.
81. Yang, J. and Y. Zhang, I-TASSER server: new development for protein structure and function predictions. *Nucleic acids research*, 2015. 43(W1): p. W174-W181
82. Mulder, N.J. and R. Apweiler, Tools and resources for identifying protein families, domains and motifs. *Genome biology*, 2001. 3(1): p. 1-8.
83. Kim, S., et al., PubChem Substance and Compound databases. *Nucleic Acids Res*, 2016. 44(D1): p. D1202-13.
84. Kumar, N., et al., Preclinical evaluation and molecular docking of 1, 3-benzodioxole propargyl ether derivatives as novel inhibitor for combating the histone deacetylase enzyme in cancer. *Artificial cells, nanomedicine, and biotechnology*, 2018. 46(6): p. 1288-1299.
85. Daina, A., O. Michielin, and V. Zoete, SwissADME: a free web tool to evaluate pharmacokinetics, drug-likeness and medicinal chemistry friendliness of small molecules. *Scientific reports*, 2017. 7: p. 42717-42717.
86. Pires, D.E., T.L. Blundell, and D.B. Ascher, pkCSM: predicting small-molecule pharmacokinetic and toxicity properties using graph-based signatures. *Journal of medicinal chemistry*, 2015. 58(9): p. 4066- 4072.
87. Morris, G.M., et al., AutoDock4 and AutoDockTools4: Automated docking with selective receptor flexibility. *Journal of computational chemistry*, 2009. 30(16): p. 2785-2791.
88. C, S., et al., Molecular docking, validation, dynamics simulations, and pharmacokinetic prediction of natural compounds against the SARS-CoV-2 main-protease. *Journal of Biomolecular Structure and Dynamics*, 2020: p. 1-27.

89. Laskowski, R.A. and M.B. Swindells, LigPlot+: multiple ligand-protein interaction diagrams for drug discovery. *J Chem Inf Model*, 2011. 51(10): p. 2778-86.
90. Umar, A.B., et al., Docking-based strategy to design novel avone-based arylamides as potent V600E- BRAF inhibitors with prediction of their drug-likeness and ADMET properties. *Bulletin of the National Research Centre*, 2020. 44(1): p. 179-183.
91. Cinar, M.G., et al., Effect of dietary vitamin E supplementation on vascular reactivity of thoracic aorta in streptozotocin-diabetic rats. *Pharmacology*, 2001. 62(1): p. 56-64.
92. Kim, Y.-S., et al., Antihyperlipidemic and antioxidant effects of Insamsansaeum (Renshenshanzha-yin) in hypercholesterolemic rats. *The Journal of Korean Medicine*, 2006. 27(4): p. 96-104.
93. Ulker, S., P.P. McKeown, and U. Bayraktutan, Vitamins reverse endothelial dysfunction through regulation of eNOS and NAD(P)H oxidase activities. *Hypertension*, 2003. 41(3): p. 534- 539.
94. Feig, D.I., B. Soletsky, and R.J. Johnson, Effect of allopurinol on blood pressure of adolescents with newly diagnosed essential hypertension: a randomized trial. *Jama*, 2008. 300(8): p. 924-932.
95. Perez-Rodríguez, L., F. Mougeot, and C. Alonso-Alvarez, Carotenoid-based coloration predicts resistance to oxidative damage during immune challenge. *Journal of Experimental Biology*, 2010. 213(10): p. 1685-1690.
96. Rao, A.V. and L.G. Rao, Carotenoids and human health. *Pharmacol Res*, 2007. 55(3): p. 207-216.
97. Rains, T.M., S. Agarwal, and K.C. Maki, Antiobesity effects of green tea catechins: a mechanistic review. *J Nutr Biochem*, 2011. 22(1): p. 1-7.
98. Rena, G., D.G. Hardie, and E.R. Pearson, The mechanisms of action of metformin. *Diabetologia*, 2017. 60(9): p. 1577-1585.

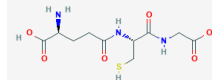
99. Abdallah, E.M., Garlic(*Allium sativum*) as antimicrobial drug: a mini-review. *Novel Approches in Drug Designing and Develop*, 2017. 3(2): p. 1-5.

# Appendix A

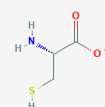
TABLE 1: Ligands name, molecular formula, weight, and molecular structure [71].

S. No	Name	Molecular Formula	Weight (g/mol)	Molecular Structure
1	3-(Allylsulphinyl)-L-alanine	$C_6H_{11}NO_3S$	177.22	
2	Allicin	$C_6H_{10}OS_2$	162.3	
3	Diallyl sulfide	$C_6H_{10}S$	114.21	
4	Diallyl disulfide	$C_6H_{10}S_2$	146.3	
5	Diallyl trisulfide	$C_6H_{10}S_3$	178.3	

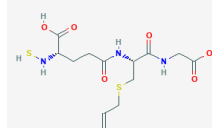
6 Glutathione  $C_{10}H_{17}N_3O_6S$  307.33



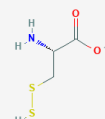
7 L-Cysteine  $C_3H_7NO_2S$  121.16



8 S-allyl-mercapto  
-glutathione  $C_{13}H_{21}N_3O_6S_2$  379.5



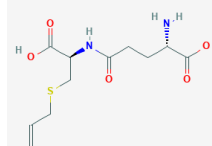
9 Thiocysteine  $C_3H_7NO_2S_2$  153.23



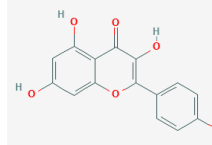
10 gamma-glutamyl-  
L-cysteine  $C_{16}H_{27}N_7O_5S$  429.5



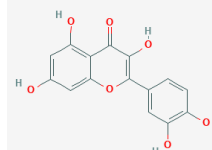
11 gamma-Glutamyl-  
S-allylcysteine  $C_{11}H_{18}N_2O_5S$  290.34



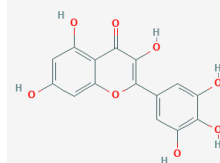
12 Kaempferol  $C_{15}H_{10}O_6$  286.24



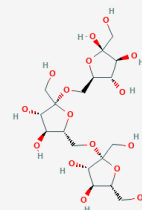
13 Quercetin  $C_{15}H_{10}O_7$  302.23



14 Myricetin  $C_{15}H_{10}O_8$  318.23



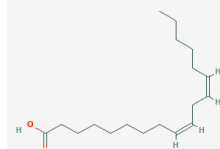
15 fructan  $C_{18}H_{32}O_{16}$  504.4



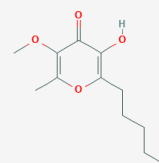
16 Lauric acid  $C_{12}H_{24}O_2$  200.32



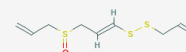
17 Linoleic acid  $C_{18}H_{32}O_2$  280.4



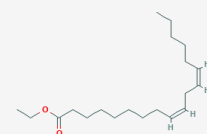
18 Allixin  $C_{12}H_{18}O_4$  226.27



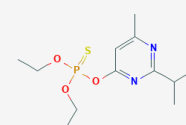
19 ajoene  $C_9H_{14}OS_3$  234.4



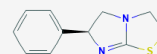
20 Ethyl linoleate  $C_{20}H_{36}O_2$  308.5



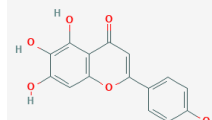
21 Diazinon  $C_{12}H_{21}N_2O_3PS$  304.35



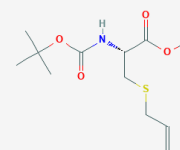
22 Levamisole  $C_{11}H_{12}N_2S$  204.29



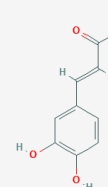
23 Scutellarein  $C_{15}H_{10}O_6$  286.24



24 S-allylcysteine methylester  $C_{12}H_{21}NO_4S$  275.37



25 Caffeic acid  $C_9H_8O_4$  180.16



# Appendix B

TABLE 2: Ligands, hydrogen bonds, hydrophobic interactions obtained by ligplot [72, 73].

Sr. No	Name	No of HBs	Amino Acids	Hydrogen Bonding Distance	Hydrophobic Bonding
1	3-(Allylsulphinyl)-L-Alanine	4	Asn151	2.96	Gln110
			Asp295	2.94	Phe8
			Arg298	2.96	
			Thr111	3.07	
2	Allicin	0			Gln110 Val202
3	Diallyl Sulfide	0			Asn203 Val202 Gln110
					Asn214
					His246 Val202 Gly109 Thr292 Pro293 Pro108 Ile249
4	Diallyl Disulfide	0			
5	Diallyl Trisulfide	0			



					Phe294
					Asn203
6	Glutathione	4	Gln110	2.93	Ile152
			Asn151	2.98	Phe8
			Thr111	2.68	Phe294
			Arg298	3.01	Asp153
					Asp295
					Thr292
7	L-Cysteine	3	Thr292	3.02	Gln110
			Thr111	3.23	Phe294
			Asn151	3.28	Arg298
					Asp295
8	S-Allyl-Mercapto- Glutathione	2	His41	3.13	Ser46
			Thr25	3.03	Met49
					Cys44
					Thr45
9	Thiocysteine	0			Asn214
10	Gamma-Glutamyl- L-Cysteine	5	Phe294	3.22	Val202
			Asn151	3.02	His246
			Thr111	2.84	Ile200
			Asp295	3.19	Glu240
			Arg298	3.02	Pro108
					Pro132
					Gln110
					Gly109
					Phe8
11	Gamma-Glutamyl- S-Allylcysteine	0			Asn214
12	Kaempferol	4	Gln110	2.93	Ile152

			Asn151	2.98	Phe8
			Thr111	2.68	Phe294
			Arg298	3.01	Asp153
					Asp295
					Thr292
13	Quercetin	2	Gly109	3.11	Gln110
			Asn203	3.03	Val202
					Ile200
14	Myricetin	5	Thr292	3.05	Asn151
			Thr111	2.72	Phe305
			Ile152	3.13	Asp153
			Asp295	3.87	Val303
			Gln110	3.29	Arg298
					Phe294
15	Fructan	5	Thr111	3.26	Ile152
			Asp295	2.7	Phe8
			Ser158	2.91	Ile106
			Asn151	3.11	Val104
			Gln110	3.01	Asp153
16	Lauric Acid	2	Leu110	3.31	Asn151
			thr111	3.1	Asn203
					Val202
					Pro108
					Gly209
17	Linoleic Acid	1	His246	3.03	Ile152
					Phe8
					Gln110
					Pro108
					Val202
					Gly109

---

					Asn203
					Asn151
18	Allixin	2	Asn203	2.91	Pro108
			His246	3.17	Pro293
					Thr292
					Gly109
					Ile200
					Ile249
					Gln110
					Val202
					Phe294
19	Ajoene	0			Pro132
					Pro293
					Pro108
					Thr292
					Gly109
					Ile200
					Ile249
					Glu240
					His246
					Val202
					Phe294
20	Ethyl Linoleate	1	His246	3.27	Pro293
					Pro108
					Thr292
					Gly109
					Ile152
					Ile200
					Glu240
					Val202
					Phe294

					Phe8
					Gln110
					Asn151
					Asn203
					Arg298
21	Diazinon	0			Gln110
					Gln107
					Val202
					Gly109
					Ile200
					Glu240
					Pro108
22	Levamisole	0			Gln110
					Val202
					Gly109
					Ile200
					Glu240
					Pro108
					Pro132
23	Scutellarein	2	Thr111	3.26	Asn151
			Gln110	3.3	Asp153
24	S-allylcysteine methylester	1	His246	3.24	Gln110
					Val202
					Gly109
					Ile200
					Glu240
					Pro108
					Pro132
25	Caffeic acid	2	Asn151	3.18	Gln110

Thr111 3.01

---

# Appendix C

TABLE 3: Absorption among different ligands [86].

Ligand	Water Solubility	CaCO <sub>2</sub> Permeability	Intestinal Absorption (human)	Skin permeability	P-glu-coprotein substrate	P-glu-coprotein I inhibitor	P-glu-coprotein II inhibitor
3-(Allylsulphanyl)-L-Alanine	-2.888	0.619	76.495	-2.735	No	No	No
Allicin	-1.72	1.316	96.229	-1.877	No	No	No
Diallyl Sulfide	-2.695	1.394	96.268	-1.488	No	No	No
Diallyl Disulfide	-3.222	1.399	94.769	-1.429	No	No	No
Diallyl Trisulfide	-3.781	1.403	92.573	-1.449	No	No	No
Glutathione	-2.892	-0.536	0	-2.735	Yes	No	No
L-Cysteine	-2.888	0.386	74.807	-2.737	No	No	No

S-Allyl-Mercapto-Glutathione	-2.205	-0.457	0	-2.735	Yes	No	No
Thiocysteine	-2.887	0.424	78.653	-2.737	No	No	No
Gamma-Glutamyl-L-Cysteine	-2.892	-0.598	0.259	-2.735	Yes	No	No
Gamma-Glutamyl-S-Allylcysteine	-2.891	-0.517	8.312	-2.735	Yes	No	No
Kaempferol	-3.04	0.032	74.29	-2.735	Yes	No	No
Quercetin	-2.925	-0.229	77.207	-2.735	Yes	No	No
Myricetin	-2.915	0.095	65.93	-2.735	Yes	No	No
Fructan	-1.2	-0.835	0	-2.735	Yes	No	No
Lauric Acid	-4.181	1.562	93.379	-2.693	No	No	No
Linoleic Acid	-5.862	1.57	92.329	-2.723	No	No	No
Allixin	-3.074	1.301	93.438	-3.141	No	No	No
Ajoene	-3.54	1.329	95.186	-1.745	No	No	No
Ethyl Linoleate	-7.525	1.608	92.241	-2.774	No	No	Yes
Diazinon	-3.757	1.509	92.749	-3.005	No	No	No
Levamisole	-3.173	1.491	93.678	-2.075	No	No	No
Scutellarein	-3.156	-0.357	66.687	-2.735	Yes	No	No

---

S-allylcys-							
teine meth-	-2.213	0.986	93.247	-3.061	No	No	No
ylester							
Caffeic							
acid	-2.33	0.634	69.407	-2.722	No	No	No

---